Journal of Environmental Radioactivity 216 (2020) 106160

Contents lists available at ScienceDirect

Journal of Environmental Radioactivity

journal homepage: http://www.elsevier.com/locate/jenvrad

Radioactive particles released from different sources in the Semipalatinsk Test Site

S. Lukashenko [a,b], A. Kabdyrakova [c], O.C. Lind [b,*], I. Gorlachev [d], A. Kunduzbayeva [c], T. Kvochkina [d], K. Janssens [e], W. De Nolf [f], Yu. Yakovenko [c], B. Salbu [b]

[a] Russian Institute of Radiology and Agroecology, Obninsk, Russia
[b] CERAD CoE, Norwegian University of Life sciences, Faculty for Environmental Sciences and Nature Research Management, Aas, Norway
[c] Institute of Radiation Safety and Ecology, NNC, Kurchatov, Kazakhstan
[d] Institute of Nuclear Physics, Almaty, Kazakhstan
[e] AXES, Department of Physics, University of Antwerp, Groenenborgerlaan 171, B-2020 Antwerp, Belgium
[f] European Synchrotron Radiation Facility, Avenue des Martyrs 71, 38043 Grenoble Cedex 9, France

ARTICLE INFO

Keywords:
Nuclear tests
Radioactive particle characterization
SR-μ-XRF/XRD
Particle size
Mobility

ABSTRACT

A total of 456 nuclear tests were performed from 1949 to 1989 at the Semipalatinsk Test Site (STS) in Kazakhstan, as part of the nuclear weapon test program of the USSR. To identify if radionuclides such as ^{137}Cs, ^{90}Sr, ^{241}Am, ^{239} ^{240}Pu were associated with radioactive particles, soil samples were collected at selected contaminated sites (i.e. Experimental field, Excavation sites, Fallout plume sections, Background global fallout area, and Degelen Mountain) within the STS. A series of techniques have been applied to identify the size distributions of radionuclides, the prevalence of radioactive particles in soils, and the degree of leachability of particle associated radionuclides by different agents. In addition, selected particles were characterized non-destructively using digital autoradiography, environmental scanning electron microscopy (ESEM) and synchrotron radiation microscopic X-ray techniques. Radioactive particles were identified at all sites; large vitrified particles were identified at epicenters, and the size of particles decreased along the plume with distance from the epicenters. The radioactive particles identified varied in composition, size and leachability. In general, ^{137}Cs, ^{241}Am, ^{239} ^{240}Pu were strongly associated with solid phases (90–99%) in soils, while ^{90}Sr exhibited much greater variability. The fraction of ^{90}Sr present in exchangeable forms was low close to epicenters, while the extractability increased along the plume as the particle size distribution decreased.

The results suggest that at least four different types of radioactive particles are present at STS: 1) Relatively large spherical particles with a shiny glazed, melted surface with internal porous structure, and surface layers enriched in transuranic elements, identified at epicenters of detonations, 2) Vitrified irregular particles probably originating from debris of nuclear device with interactions from soil components, also identified at epicenters of detonations, 3) Particles with visually unchanged structure, containing micro-inclusions of fissile materials associated with soil components, also identified at epicenters; 4) Particles with amorphous structures associated with underground detonations, identified in soil in the vicinity of the entrance of the detonation tunnels at the Degelen Mountain. These were probably formed by secondary mechanisms due to sorption and fixation of radionuclides. Thus, the present work shows that the STS should be considered an important observatory site to link particle characteristics to specific sources and to release conditions as well as to ecosystem transfer of particle associated radionuclides.

1. Introduction

The Semipalatinsk Test Site (STS), located in the North-East of Republic of Kazakhstan, was the first and the main proving grounds for the testing of nuclear weapons by the former Soviet Union. The test site, situated 150 km west of Semey city, extends over an area of 18,300 km^2 i.e., a territory comparable in size to Slovenia. The site is characterized as a flat landscape typical of the plains of the dry Eurasian steppe. A total

* Corresponding author.
E-mail address: ole-christian.lind@nmbu.no (O.C. Lind).

https://doi.org/10.1016/j.jenvrad.2020.106160
Received 31 May 2019; Received in revised form 7 January 2020; Accepted 8 January 2020
Available online 26 February 2020

of 456 nuclear weapon tests (616 nuclear devices) were performed from 1949 until 1989, including atmospheric air-drop or tower shots and underground shots in boreholes and tunnels. The first bomb was conducted in 1949 from a tower at the "Experimental field" at STS. Then, the majority of tests was performed before 1963 (Test ban treaty), when the atmospheric tests were replaced by underground nuclear explosions (Lukashenko et al., 2017, Nazarbayev et al., 2016).

During 1949–1962, a total of 116 atmospheric tests were performed at the Experimental field site with the purpose to study the effects of nuclear detonations. Of them, 30 were ground tests and 86 were detonated above ground, i.e., from towers or as airdrops. From 1961, 340 underground nuclear explosions were performed within the STS (Fig. 1).

The tunnels at the "Degelen Mountain" site were used for 209 tests such as underground explosions of nuclear warheads and devices, and large-scale testing of underground engineering constructions and technological equipment. Underground nuclear weapon tests were also performed at the Balapan (105 tests), Sary-Uzen (24 tests) and Telkem (2 excavation tests) sites with the purpose to test nuclear warheads and devices, to run large-scale tests of strategic objects such as missile silos (sometimes also equipped with the missiles), to test unified command bunkers, nuclear weapons storages and their technological equipment, as well as to develop technologies for industrial use. Technologies were developed for utilization of underground nuclear explosions for construction of artificial water reservoirs, channels, for seismic probing for minerals exploration, for construction of underground storage vessels and to develop methods to extinguish oil fires etc. During the STS operation, 7 nuclear explosions were performed as part of the Nuclear Explosions for the National Economy program, so-called Peaceful Nuclear Explosions (PNE) (Fig. 1). The explosion in the borehole 1004 having the purpose to construct the artificial "Atomic" Lake showed, however, that the harm from contamination associated with underground nuclear explosions could by far exceed the economic benefit.

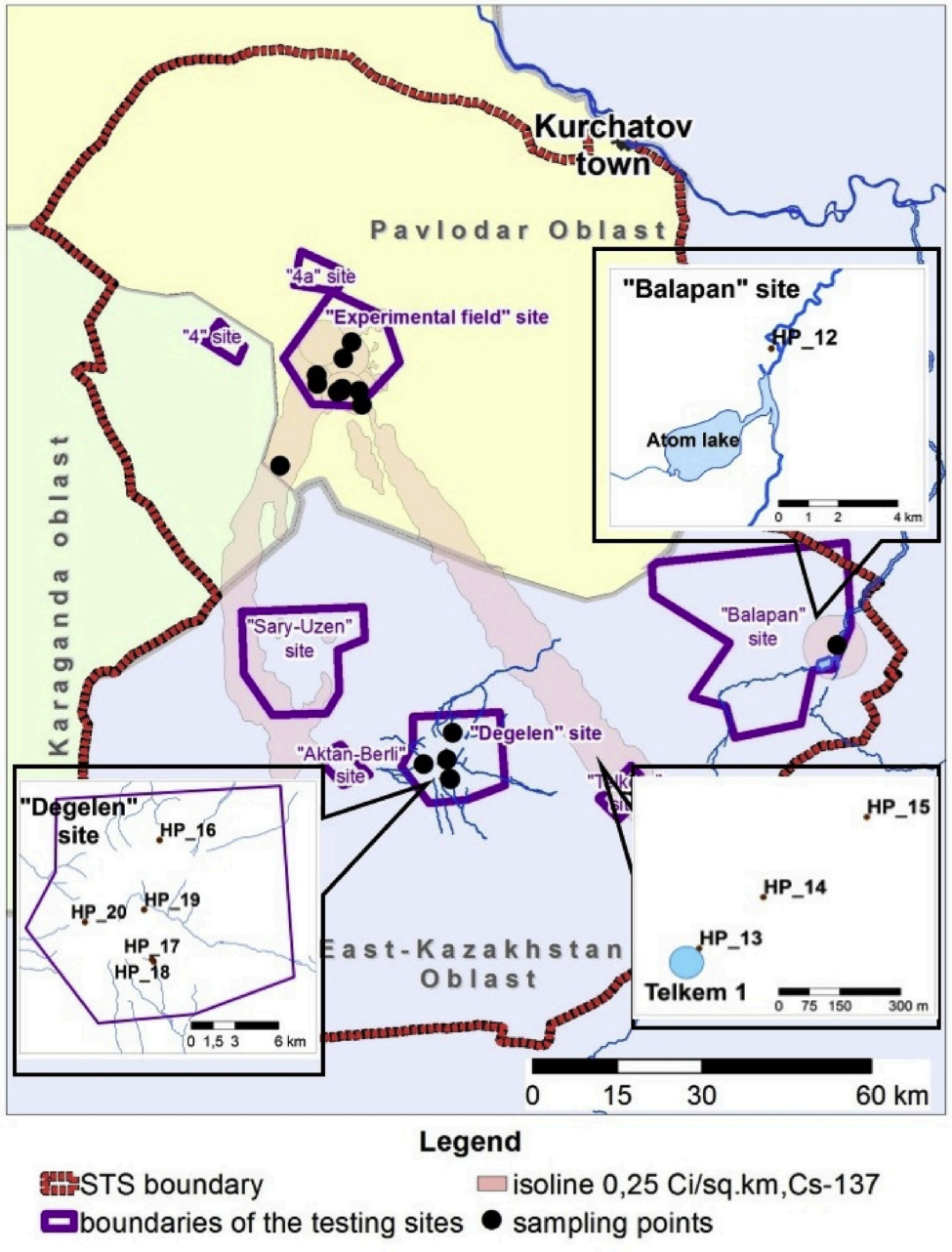

Fig. 1. Overview map of the Semipalatinsk Test Site (Lukashenko et al., 2017). Inserted maps show where radioactive particles are investigated in the present work.

Another focus area of research at the STS was subcritical experiments performed at the sites Aktan-Berli and P-2G. Along with nuclear explosions, tests of solid or liquid radioactive substances were also performed at the testing grounds "4" and "4a", and in total 175 blasts employing conventional chemical explosives were performed (Fig. 1).

From 1997 to present, the General Assembly of the United Nations (UNGA) has adopted 9 resolutions on international cooperation and coordination for the restoration of the environment and rehabilitation of the population in the Semipalatinsk region. The UNGA resolutions on the Semipalatinsk region are a clear indication of serious concerns by the international community about the long-term environmental and health impact of nuclear tests conducted at STS. Following the detonation of many different sources at the STS during the years, a series of radionuclides associated with weapon materials such as U and Pu-isotopes as well as fission products such as ^{137}Cs and ^{90}Sr isotopes, have been released to the environment. Due to the blast conditions such as high temperature and pressure, refractory elements are expected to be released as particles, ranging from submicrons to fragments, while such particles would be depleted in volatile radionuclides. Thus, the characteristics of radioactive particles such as radionuclide or elemental composition, particle size distribution, crystalline structures and oxidation states will depend on the source and the release scenario. The STS should therefore represent a unique environmental laboratory where radioactive particles from different sources could be identified. Although the source terms at STS are very complex, and particle weathering and radionuclide species would redistribute over time, the objective of this work is to summarize information on radioactive particles released to selected sites within STS, based on available data and recent research.

2. Material and methods

2.1. Study areas

In the present work, soil samples have been collected from within the main testing site of the STS; at the Experimental Field, Atomic Lake and the background areas as well as from the Degelen Mountain (Fig. 1, S1).

2.1.1. The Experimental Field

The Experimental Field is a flat landscape area, surrounded with low mountains towards the south, west and north. The site is approximately 300 km^2 with a perimeter of 64 km. Surface and atmospheric nuclear tests have been conducted at this site during 1949–1962. In total, 30 surface tests (including 5 cases in which the nuclear charge did not explode) and 86 atmospheric tests were conducted. For testing purposes, sites P-1, P-2, P-3, P-5 and P-7 were used (Fig. 2 and S2). Based on aerial radiological survey of the Experimental Field site during 2012–2014 (Fig. 2 and Fig S2), 24 venues of nuclear tests were identified (Lukashenko et al., 2017).

The radioactive contamination of soils at the Experimental Field can be categorized as follows:

1. Epicenters i.e., downstream and upstream the ground zero (point of explosion) with round-shaped local contamination spots with a diameter ranging from several dozens of meters to several kilometers depending on the yield of the tests.
2. Radioactive fallout plumes from surface and atmospheric nuclear tests.
3. Non-nuclear tests i.e., experiments with very low or without nuclear yield with local contaminated zones without a clear form.
4. Radioactive fallout plumes from non-nuclear experiments with nuclear materials, i.e., subcritical tests without nuclear yield.

All identified epicenter areas have common features such as: 1) the 2D distribution of radioactive contamination at the test venue has a clear round shape; 2) the specific activity of nuclear explosion derived radionuclides (fission products, activation products, transuranics) decreased exponentially from the epicenter to the boundary of the radioactive contamination zone. At present, the radioactive contaminations at the epicenter areas are represented by fission products such as ^{137}Cs, ^{90}Sr, activation products such as ^{60}Co, Eu, ^{3}H isotopes, and radionuclides associated with fissile material such as ^{239} ^{240}Pu, ^{235}U, ^{241}Am.

Radioactive fallout plumes from low-yield nuclear tests occupied an extensive area; the width of plumes ranged from several hundred meters to ~10 km, depending on yield of conducted tests and meteorological conditions at the moment of tests. Approximately 30% of the Experimental Field area is contaminated with ^{137}Cs at levels significantly higher than global fallout.

Fallout plumes from subcritical (hydrodynamic) tests represent spots with deposition of radioactive particles at the soil surface along a thin stripe starting at the experiment venue. This type of radioactive contamination has several specific features, allowing to distinguish this fallout from that of nuclear explosions as follows:

Fallout plumes of subcritical tests are much smaller than the plumes of typical nuclear tests. These plumes can be up to 3–5 km long and less than 100 m wide. The width remains virtually unchanged along the plumes.

The contamination has a specific isotopic composition related to the nuclides associated with the detonating source. No other radionuclides (fission and activation products, such as ^{137}Cs, ^{90}Sr, ^{60}Co, ^{152}Eu and etc.) are present or their concentrations are insignificant.

Investigation of the size distribution (granulometric fractions) of radionuclides in soils from epicenter areas was based on samples from three technical sites (P-1, P-5, P-2/P-7) at the Experimental Field (Fig. 2 and Fig S2). In total, 9 soil samples (2–3 samples at each point) were studied. To identify changes in radionuclide species distribution along a local test plume, samples were collected from the fallout plume at the B-1site, a low-yield surface explosion (Fig. 3). Soil samples (10 10 cm and 0–5 cm depth) were collected using the "envelope" method, i.e. one sample from the centre and from each corner of a square (1 1 m^2).

Radioactive particles were investigated in samples from the epicenter zones (HP-08 - HP-10) and from the fallout zones (HP-02, HP-04) as illustrated in Fig. 2.

2.1.2. Excavation explosion at Atomic Lake

The first underground explosion with ground outburst (excavation explosion) at the STS took place at Balapan in 1965 in borehole N–1004. The test was designed to obtain information on the use of nuclear explosions for creating water reservoirs in arid zones. The yield of the explosion was 130 kT (93% thermonuclear, 7% fission). As a result of this explosion, a water reservoir with the depth of 100 m, named Atomic Lake, was formed at the junction of the Shagan and Ashisu rivers. At the Atomic Lake, sampling points with maximum radioactive contamination were selected, i.e., sampling was performed along the fallout plume (Fig. 4).

Soil samples were collected at the depth of 0–5 cm using the envelope method in 60–400 m intervals consequentially with distance from the ridge of the Atomic lake crater. To identify radioactive particles, a ridge sample (HP-11) and a sample 50 m from the ridge in the North-East direction (HP-12) were collected (Fig. 1).

2.1.3. Radioactive plumes crossing territories contaminated with global fallout

In 2007, regular radioecological research was initiated of the entire test site area, except for all technical sites previously used for nuclear tests (e.g., Experimental Field, Atomic Lake, Degelen Mountain) to determine the background contamination level due to global fallout. Based on air gamma survey conducted already in 1991 (Fig. 1, Lukashenko et al., 2017), two plumes («southern» and «southeastern») were

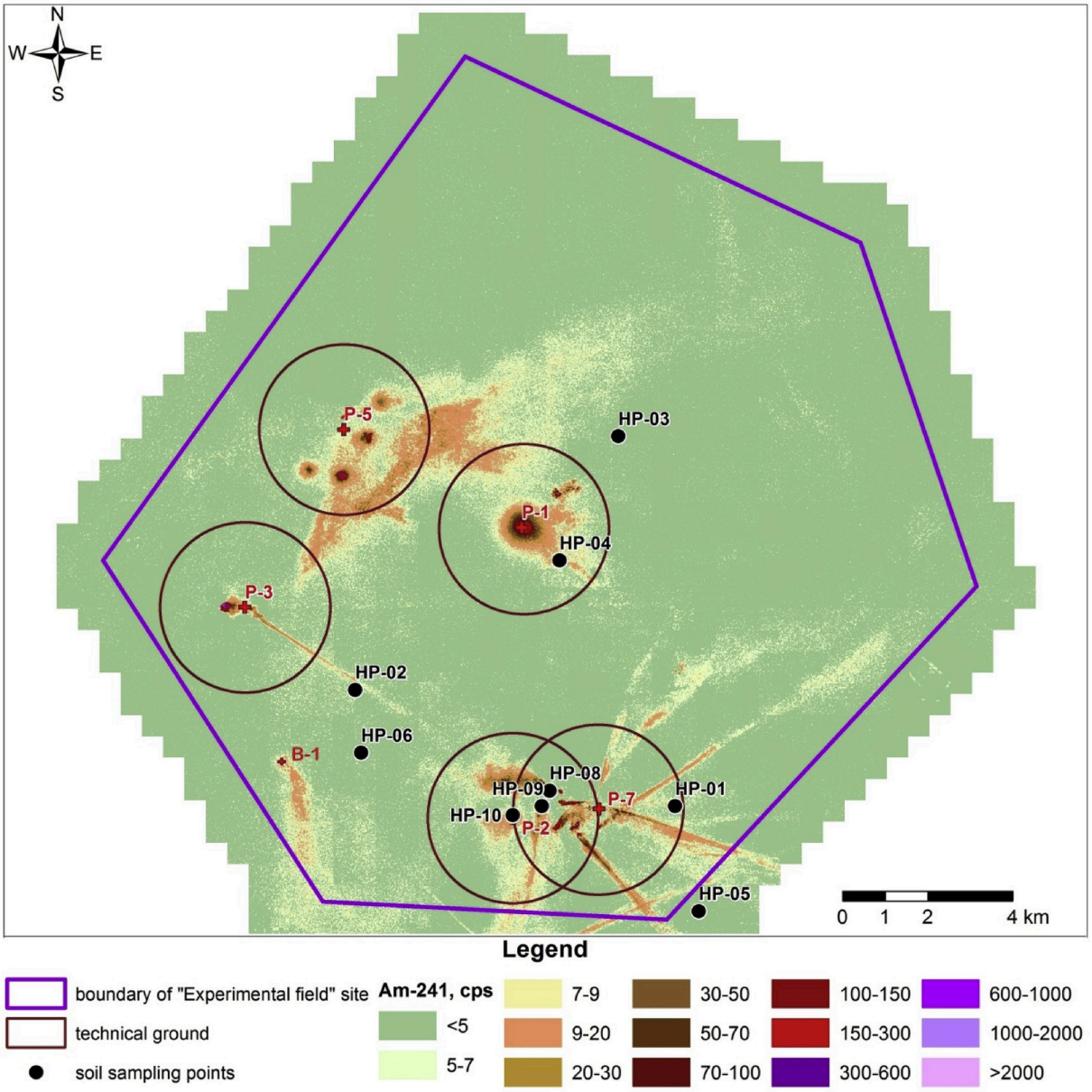

Fig. 2. Map of the Experimental Field showing the ^{241}Am contamination (counts per second; cps), sites of soil sampling and sites at which radioactive particles (HP) were collected (Lukashenko et al., 2017).

identified crossing the global fallout STS territories. The Northern part of the background area at the STS is believed to be contaminated by global fallout only, while the Southeastern parts of the background area at STS territory is expected to be partially affected by fallouts from the plume of the thermonuclear test with the yield of 400 kT conducted in the 1953 at the Experimental Field site.

Characteristics of the radioactive fallout plumes at STS refer to the composition and radionuclide speciation, levels of radionuclide activity as well as the width and length of the plume. The composition refers to fission products (^{137}Cs and ^{90}Sr) and transuranics (^{241}Am, $^{239\ 240}$Pu, ^{241}Pu), while almost no activation products (Eu-isotopes and ^{60}Co) isotopes were identified. The width of such plumes is ranging from 10 to 14 km, while the length of plumes exceeds 100 km, however, the real lengths are still to be accurately determined.

The plumes can be differentiated based on the isotope ratios of ^{90}Sr/^{137}Cs and $^{239\ 240}$Pu/^{241}Am, which are characteristics for each plume. At a distance of about 100 km from the test venue, radionuclide activity ratios in soils are: in the "southern" plume ^{90}Sr/^{137}Cs ratio equals 0.7 and $^{239\ 240}$Pu/^{241}Am equals 13.3; in the "south-eastern" plume ^{90}Sr/^{137}Cs ratio equals 3.0 and $^{239\ 240}$Pu/^{241}Am equals 12.0.

Soil samples were collected using "envelope" method at the depth of 0–5 cm in points of increased soil activity concentrations, and also directly at the thermonuclear explosion fallout plume, running through the background area of southeastern part of the STS (Fig. 1). For the study of radioactive particles, the points were selected at areas without obvious influence from nuclear explosions (HP-01, HP-03, HP-05, HP-06).

2.1.4. Degelen Mountain

The Degelen Mountain (about 330 km^2) is located in the eponymous mountain massif in the southern part of Semipalatinsk Test Site (Fig. 1, Fig S1). The site was designed for low-yield tests (up to several dozens of kilotons) in horizontal tunnels. From 11.10.1961 to 04.10.1989, 209 tests including 2 PNEs were conducted in the 181 tunnels. At present, the main transport of radionuclides out of the epicenter area is due to groundwater seepage. Depending on the weather and year, streams

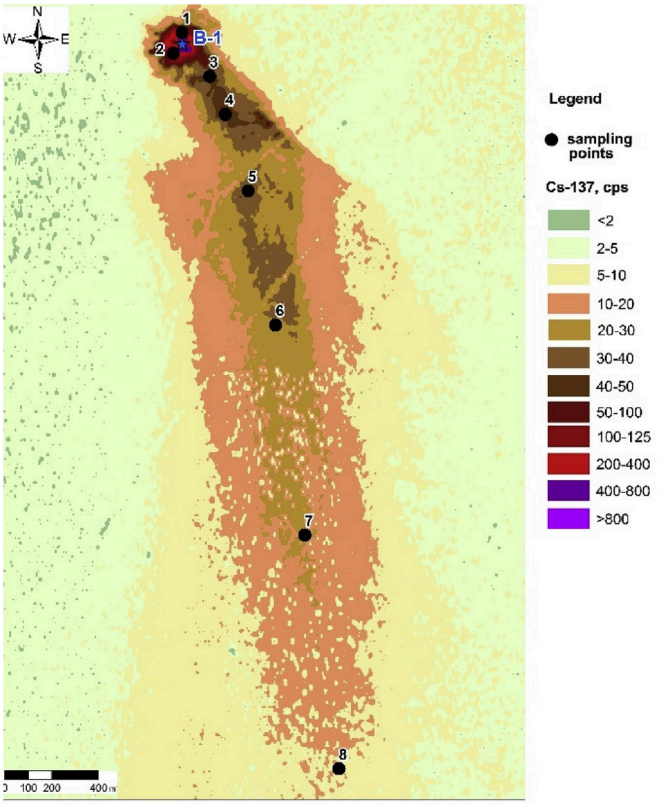

Fig. 3. Soil sampling site in the plume from the low yield test at object "B-1" (Lukashenko et al., 2017).

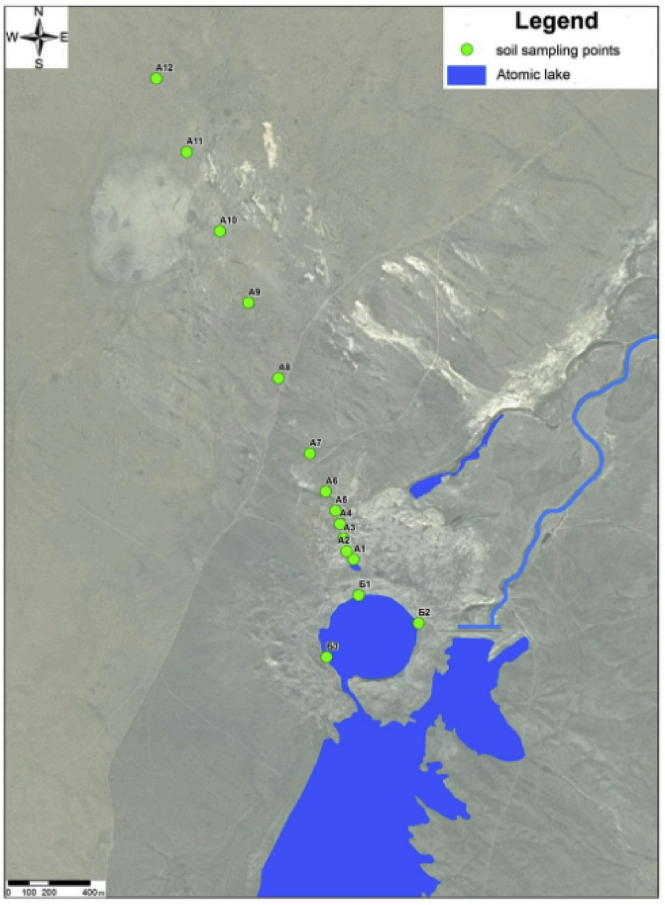

Fig. 4. Soil sampling sites at the Atomic lake (Lukashenko et al., 2017).

flowing through 8 to 12 of the testing sites contribute to weathering of contaminated solid phases such as melted soil and rock, and to potentially mobilizing radionuclides to the environment downstream the tunnels. These radionuclides may sorb to sediments, giving rise to up to 1 10^4 Bq/kg ^{239} ^{240}Pu, 10^5 Bq/kg ^{90}Sr, and 10^6 Bq/kg ^{137}Cs in stream sediments with maxima usually found near the tunnel entrances, and rapidly decreasing with distance from the tunnels. The width of radionuclide distribution in lateral direction depended on the width of the watercourse and was limited by the landscape. The width of these watercourses usually did not exceed 3–5 m (Lukashenko, 2017).

At the Degelen Mountain site, samples were collected from the vicinity of the entrance to tunnel N– 176, a tunnel which has been exposed to water from a stream flowing through the site for more than 20 years. Samples (0–20 cm) were collected at individual spots in flooded stream embankments outside the tunnel entrance (Fig. 5). To identify radioactive particles, soil samples were collected at the vicinity of the entrances of the tunnels N– 139 (HP-16), N– 609 (HP-17, HP-18), N– 177 (HP-19), and N– 503 (HP-20). Tunnels N– 609, 177 and 503 are subject to flow-through water, whereas tunnel No. 139 appeared to be dry.

2.2. Sample treatment

Soil samples were dried in a drying cabinet at maximum 60° C. Coarse stones and vegetative inclusions were removed from the dried sample, then dry samples were sieved using a 1 mm mesh sieve.

2.2.1. Particle-size fractionation of soil

To divide the soil into particle-size fractions wet sieving and sedimentation were used. Soil sample was moistened with distilled water and fractioned in porcelain mortar using pestle with rubber ending. The soil suspension was sieved using consecutive sieves with cell size of 500, 250, 100, 63, 40 μm. The suspension left after sieving (mesh 40 μm) was further separated by means of sedimentation. Soil suspension was settled into measuring flask for a certain period of time, after that the suspension above the sediment was decanted and the sediment was taken out from the bottom. Decanted suspension was transferred back to the cylinder, water level was restored, and sedimentation was repeated. The average period of suspension settling was 17 min, 1 h 10 min, and 20 h 28 min according to standard technique (GOST, 2014). The remaining fraction was separated by means of centrifugation. Thus, the fractions 40-8 μm, 8-5 μm, 5-1 μm and <1 μm fractions were collected, and the activity concentrations of radionuclides (^{137}Cs, ^{90}Sr, ^{241}Am and ^{239} ^{240}Pu) were determined in all separated fractions.

Then, the enrichment coefficients of the fractions were calculated using the following formula:

$$Ef \quad Cf/Cb,$$

where.

E_f – enrichment (depletion) factor;

C_f – the concentration of radionuclides in a certain size fraction;

C_b – the concentration of radionuclides in the total (bulk) sample.

2.2.2. Sequential extraction of radionuclides in soil

Selected soil samples were subjected to a sequential extraction procedure in order to distinguish between the reversible and irreversible interactions of radionuclides with solid phases. The sequential extraction protocol was based on that of Pavlotskaya (1974), provided for determination of water-soluble, exchangeable (mobile and tightly bound) and non-exchangeable species of radionuclide in soils (Tab. S1). In some cases, the procedure was modified by adding 0.1 NaOH as an intermediate stage to obtain information on organically bound fraction of radionuclides, based on a technique developed by Tyurin (Ponomaryova and Plotnikova, 1980). The soil/solution ratio was 1:5 (g/ml).

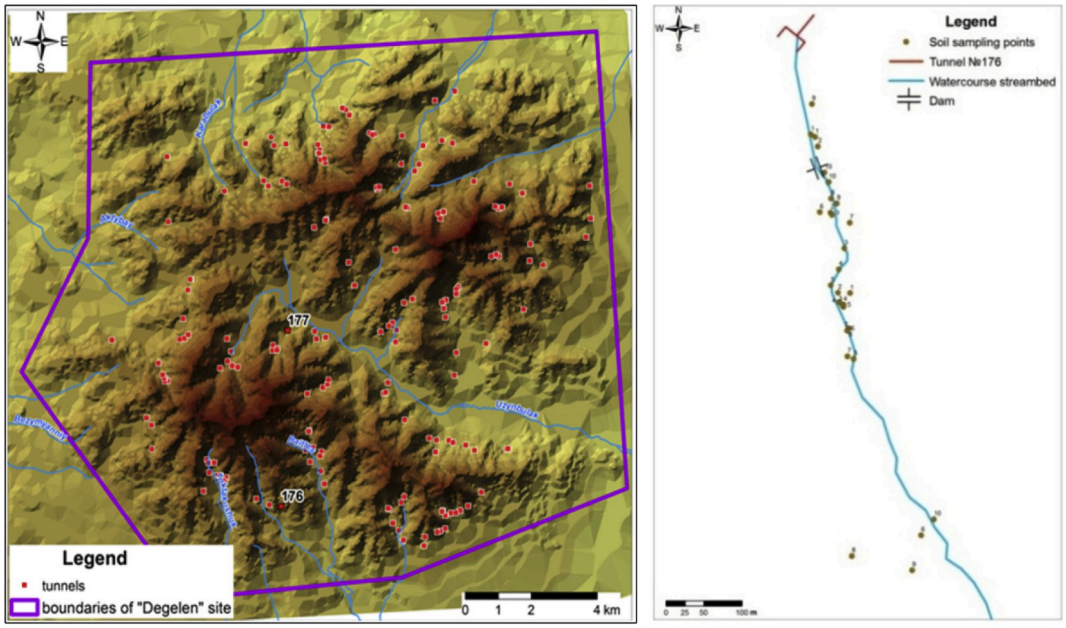

Fig. 5. The Degelen test site. Overview (left) and soil sampling sites in the area of the tunnel N– 176 (right) (Lukashenko et al., 2017).

The suspension was mixed for 1 h, then the soil suspensions were filtered 16 h later through a "blue" ribbon filter. Radionuclide activity concentrations were determined in extracts and in residues. If necessary, extracts were also centrifuged prior to measurements.

2.3. Identification and isolation of radioactive particles

Various methods were used to identify and isolate radioactive particles. At NMBU, particles were identified using digital autoradiography using Imaging plates (Molecular Dynamics) and a Typhoon (GE Healthcare) scanner (Geckeis et al., 2019; Salbu and Lind, 2020), or by means of sample splitting combined with gamma spectrometry (Bunzl, 1997; IAEA, 2011). Isolated particles were fixed onto carbon double-faced sticky tape and mounted onto Al stubs for further identification of particles in Zeiss EVO 50 variable pressure Environmental Scanning Electron Microscope (ESEM) with an Inca EDX analytical system (Oxford Instruments, Oxford, UK) including a Si(Li) detector (Lind et al., 2013).

At Institute of Radiation Safety and Ecology, NNC, identification of radioactive particles in a sample was based size fractions using wet sieving on a vibrating-scattering shaker (Analysette 3, company FRITSCH) with mesh sizes 1.25, 0.50, 0.28, 0.112 0.040 mm, providing the following fractions: particle fraction 1: size > 1.25 mm, fraction 2: size 1.25 > f > 0.5 mm, fraction 3: size 0.5 > f > 0.28 mm, fraction 4: size 0.28 > f > 0.112 mm, and fraction 5:size 0,112 > f > 0.04 mm. The <0.04 mm fraction was not subjected to further investigations. After each experiment, the sieves were washed in an ultrasonic bath (Laborette 17, FRITSCH). To reduce the probability of contamination of low-level soil samples from high-level samples, the least active samples were sieved first. Two alternative approaches were used to identify and isolate radioactive particles; visual identification (microscopes) and fission track method. Wet sieving fractions of soil samples were divided, one portion (up to 200 g) was studied visually for fraction 1 (>1250 μm), fraction 2 (1250-500 μm) and fraction 3 (500-280 μm). The remaining portions (0.1–10 g) were analyzed only by means of the fission track method.

2.3.1. Induced fission tracks

Based on thermal neutrons stimulated fission, the detection of fission fragments of ^{239}Pu nuclei was performed using solid-state detectors. A large cross section of ^{239}Pu fission (σ_f 742,5 b) and the relatively high specific activity in radioactive particles allowed measurements at relatively low thermal neutrons fluxes of ~10^9-10^{10} n/(cM^2*c) from a thermal neutron generator based on the isochronous cyclotron INP U-150. Neutrons in this case were formed as a result of nuclear reactions ^{9}Be (p, xn) or ^{9}Be (d, xn), and quartz glass was used as a solid state detectors. After irradiation of the sample (a monolayer of particles of a certain fraction), detectors were treated with 35% hydrofluoric acid to manifest tracks from fission fragments. The entire area of detectors was scanned using a MBI-9 microscope at 70x magnification. For each detected cluster of tracks indicating a radioactive particle (Fig. S3), the number of tracks was counted.

2.4. Microanalytical techniques

2.4.1. Computerized submicron X-ray absorption tomography

Following particle characterization by gamma spectrometry, light microscopy and ESEM-EDX, particles were subjected to x-ray absorption tomography (SkyScan 1172 Micro-CT) with 500 nm resolution at SkyScan Ltd, Antwerpen, Belgium. The specimens were mounted on a glass capillary with super glue without further preparation and irradiated with a 80 kV x-ray beam while 2D X-ray images were recorded for every rotation. Three dimensional images and videos revealing the density distributions were reconstructed from 2600 2D projections which are then used to analyze the internal strutures.

2.4.2. Synchrotron experiments

Selected particles were subjected to combined micro-X-ray fluorescence (μ-XRF) and micro-X-ray powder diffraction (μ-XRPD) measurements, in both scanning (2D) and tomographic (3D) modes, performed on beamline L, HASYLAB synchrotron, Hamburg, Germany (Lind et al., 2013). In the present work, a focussed monochromatic X-ray microbeam of 10–15 μm diameter and with a divergence of ~4 milliradians was applied. The beam was obtained by employing a 200 period Mo/Si multilayer monochromator with mean layer thickness of 2.98 nm for energy band selection (ΔE/E 1%) and a single-bounce elliptical capillary for beam focussing (Falkenberg et al., 2004). A 1K Bruker CCD camera positioned behind the sample was used for collecting diffraction patterns in transmission mode, along with two silicon drift detectors (SDD), positioned at 90 relative to the primary X-ray beam, for

simultaneous detection of the XRF signals. For tomography, samples were scanned over a translation range (x) and a 180 rotation range (ω) with step widths Δx of 15 μm and $\Delta\omega$ of 3 , and an acquisition time of 10 s per point. Sinogram to tomogram conversion was performed by the statistical algorithm maximum-likelihood expectation maximization (MLEM) algorithm (De Nolf and Janssens, 2010). In addition to the tomographic analyses, virtual slicing was also performed in confocal mode using two polycapillary half-lenses (Janssens et al., 2004). One half-lens was used to focus the primary beam and the other half-lens was located in front of the detector, perpendicular to the first lens. The estimated depth resolution was 20–30 μm.

2.5. Determination of radionuclide concentration levels

Activity concentration of ^{137}Cs and ^{241}Am was determined by gamma-spectrometry (Canberra GX-2020 solid-state detector). Radioanalytical procedures to determine activity concentrations of ^{90}Sr as well as ^{239} ^{240}Pu included extraction of radionuclides from the soil matrix by leaching (i.e. sequential extractions) or complete decomposition with a mixture of mineral acids (HF and HNO_3), radiochemical separation and sample preparation for radiometric counting. Liquid scintillation counting ("TRICARB 3100 TR" liquid scintillation spectrometer) was used to determine ^{90}Sr in low level samples, and alpha-spectrometry was employed for Pu (Alpha – Analyst, CANBERRA, USA). For samples with relatively high ^{90}Sr activity concentrations (>100 Bq/kg), radiochemical separations were omitted and analysis was performed directly by beta-spectrometry (Progress-BG, beta-spectrometer, Russia). Quality control of the analytical work was carried out in accordance with regulations adopted in the laboratories, which includes analysis of blank samples, analysis of replicate aliquot samples (n 3) for determining of reproducibility and periodic analysis of reference materials (IAEA "Soil 6", IAEA-375). For gamma-spectrometric measurements, relative counting uncertainty was less than 10% for all samples, while for alpha - and beta-spectrometric analyses the uncertainties were about 20% for radionuclides present at activity concentrations >5 LOD Limit of Detection .

3. Results and discussions

During the last decades, information on radionuclide contaminations in the STS has been made available, for instance via comprehensive documentation from the Institute of Radiation Safety and Ecology; Kazakhstan (Lukashenko et al., 2017). In the present work, focus has been put radioactive particles produced by a number of nuclear tests, and the potential mobility and bioavailability of particle associated radionuclides of relevance for radiation impact assessments. The selected sites include epicenters within the Experimental Field, plumes from low yield detonation and from thermonuclear test contaminated a certain area within STS as well as contamination from global fallout, surface contamination from the Atomic Lake, and contamination from underground tests at the Degelen Mountain.

Generally, radioactive contamination due to fallout plumes at STS was identified in the top soil layer and approximately 90% of the radionuclides were concentrated in the top 5 cm layer of soil with activity concentrations of ^{137}Cs in this soil layer ranging from 150 to 8 10^4 Bq/kg (Lukashenko et al., 2017). Radioactive contamination at the venues for non-nuclear tests (hydronuclear and hydrodynamic experiments) was dominated by transuranics (i.e., Pu, Am), and gamma-surveys showed activity concentrations of ^{241}Am in soil exceeding n 10^4 Bq/kg. Locally, the vertical distribution of radionuclides in soils could differ from the typical distribution for radioactive fallout, and at some spots, radionuclides occur at the depth of 0,5 m. Local contamination sites in the area of safety tests (i.e., experiments without nuclear yield) are relatively small and do not exceed 100 m lengthwise.

In the present work, soils collected were separated into size fractions (wet sieved), mobility of the associated radionuclides was tested (sequential extractions) and individual particles were subjected to particle characterization techniques. Particles extracted from the Experimental field were also subjected to advanced techniques for particle characterization such as ESEM, x-ray absorption tomography with submicron resolution and synchrotron radiation based x-ray microscopic techniques.

3.1. Experimental field sites

The wide range of activity concentrations observed at the Experimental field (Fig. 2), and from the B-1 site (Fig. 3) are typical for epicenters of nuclear explosions, and significant contamination of both transuranics (Pu, Am) and fission products (Cs and Sr isotopes) are present in the soils (Table 1).

3.1.1. Size distribution fractions of radionuclides

Based on wet sieving and determination of radionuclides in obtained fraction of soils from the epicenters, enrichment factors (EF, %) for radionuclides in different size fractions are given in Fig. 6. In general, EF was relatively constant for small sized particles, while the coarse fractions larger than 250 μm were somewhat enriched in all radionuclides. For soils contaminated by plumes from low-yield nuclear tests (plume B-1), the enrichment factors for ^{137}Cs and ^{90}Sr (Fig. 7) were highest in the 500–1000 μm fraction, while the fractions 250 μm were depleted in ^{137}Cs and ^{90}Sr. Similar to EF for ^{137}Cs and ^{90}Sr, the 500–1000 μm fraction was also enriched with respect to ^{241}Am and ^{239} ^{240}Pu. In addition, the smaller fractions were enriched by ^{241}Am and ^{239} ^{240}Pu in soils from different parts of the plume. In particular, transuranic elements were enriched in the <1 μm fraction in soils collected at the end of the plume, far from the epicenters.

3.1.2. Mobility and potential bioavailability

Based on sequential extractions, the mobility and potential bioavailability of radionuclides in soils from the Experimental Field were very low due to the formation of radioactive particles from the nuclear tests (Kunduzbayeva et al., 2013; Lukashenko, 2017; Lukashenko et al., 2017). The major fraction of radionuclides in epicenter soils was strongly associated with solid phases (^{137}Cs 99%, ^{239} ^{240}Pu about 99%, ^{241}Am 90%, ^{90}Sr about 91%). Sequential extraction results showed that only a minor fraction of ^{137}Cs was associated with the exchangeable (NH_4Ac extract, 0.60%) and mobile forms (HCl extract, 0.32%). The fraction of ^{239} ^{240}Pu assumed to be associated with organic materials and in mobile forms did not exceed 0.1% and 0.4%, respectively, while ^{241}Am was more mobile than ^{239} ^{240}Pu, reaching about 8.0%. The ^{90}Sr was the most mobile radionuclide among those investigated, with a relative high fraction present in exchangeable (up to 6.0%) and mobile (up to 2.8%) forms.

In soils affected by the fallout plume from a low-yield explosion at the B-1 site (Fig. 3), the major fraction of radionuclides was also strongly associated with solid phases. A very small fraction of ^{137}Cs present in mobile forms could only be determined at the epicenter as the total activity concentration decreased rapidly with distance from the epicenter, and the mobile fraction was below detection limit. The water-soluble fraction of ^{90}Sr increased, however, in soils distant in the fallout plume (0.3–0.4%) by an order of magnitude compared with soils from the epicenter (0.03–0.05%). Similarly, the level of ^{241}Am and ^{239} ^{240}Pu

Table 1
Radionuclide concentration ranges in soil samples from the Epicenter areas and Plume B-1.

Venue	Radionuclide, Bq/kg			
	^{137}Cs	^{90}Sr	^{241}Am	^{239} ^{240}Pu
Epicenter areas	500–34,000	800–27,000	170–3700	5000–230,000
Plume B-1 (low yield)	290–590	370–1000	70–280	1700–6100

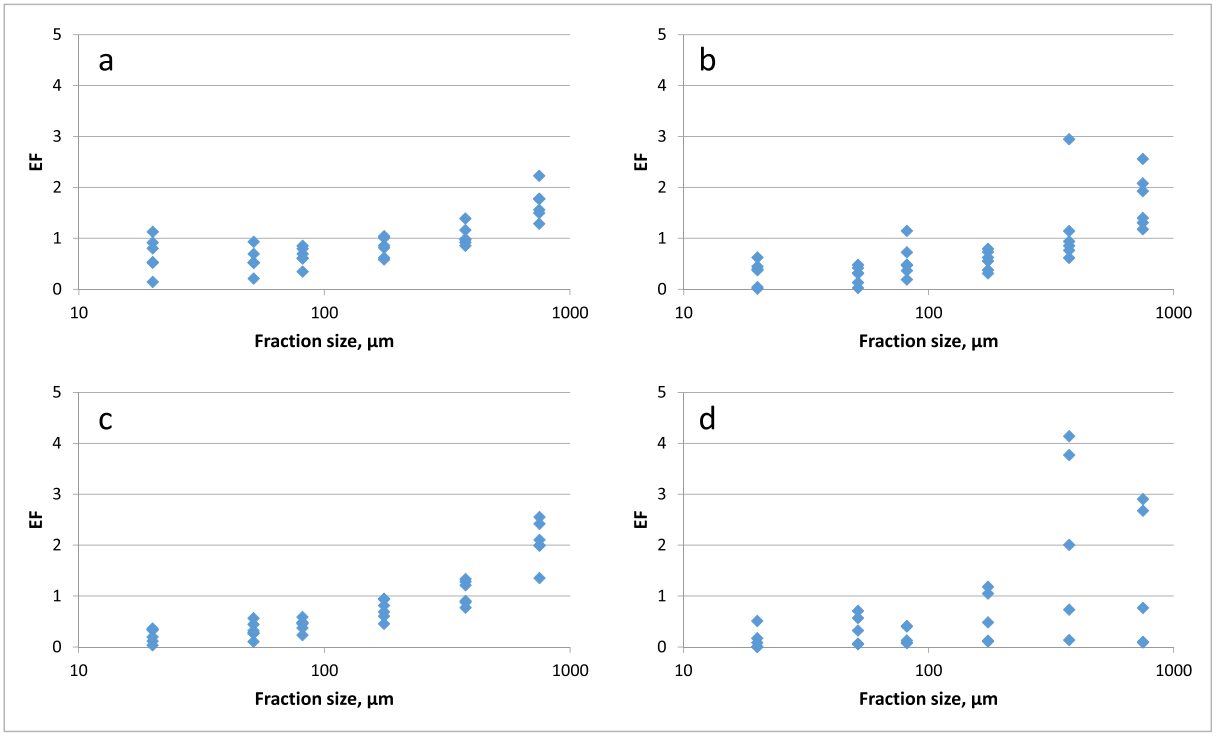

Fig. 6. Enrichment factor for ^{137}Cs (a), ^{90}Sr (b), ^{241}Am (c) and ^{239} ^{240}Pu (d) in soil fractions from epicenter of surface ground nuclear explosions.

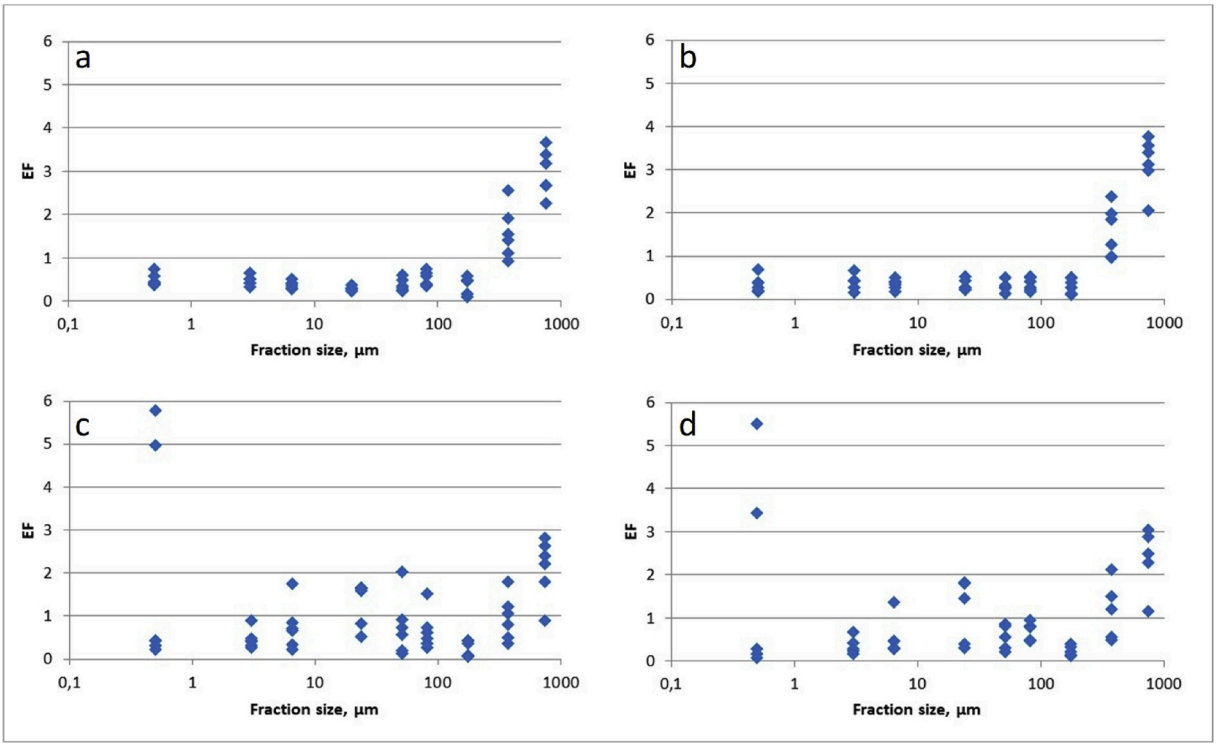

Fig. 7. Enrichment factor for ^{137}Cs (a), ^{90}Sr (b), ^{241}Am (c) and ^{239} ^{240}Pu (d) in soil fractions from the B-1 plume.

decreased according to the distance from the epicenter. The mobility (HCl extraction) of ^{239} ^{240}Pu increased at points most distant from the epicenter compared to epicenter areas. The ^{241}Am in soils at the epicenter was predominantly associated with solid phases (82%). A similar pattern was observed at the sampling points 1–6 (Fig. 3), while the mobility increased sharply at points 7 and 8. Here, the fraction of strongly associated to solids were reduced to 28–39%, with increase in the relative fraction of exchangeable (43%) and mobile forms. Throughout the fallout plume with increasing distance from the explosion epicenter, the fraction of strongly bound form of ^{239} ^{240}Pu decreased from 87 - 92% to 57–79%. At distant points of the plume, the water-soluble fraction increased from 0.01% to 0.3–0.7%, of

exchangeable form from 0.01%-0.3% to 0.9%-14%, mobile form from 0.3 - 0.6% to 0.4–1.3%, and fixed form from 7-13% to 19–27% compared to epicenter points.

3.1.3. The presence of radioactive particles

Radioactive particles have previously been observed in soils from Experimental Field at STS (Gorlachev et al., 2011). Table 2 shows the activity concentration of radionuclides in soil samples from which radioactive particles were further isolated. Table 3 shows the number of radioactive particles per gram soil, based on visual inspection with microscope and fission track. The graph "N" shows the average number of particles detected in soils using the two methods, and the average activity associated with these particles.

It should be noted that despite the proximity of the HP-08 and HP-10 sampling sites, the contamination originated from three different events. Thus, the characteristics of identified radioactive particles could vary significantly. At HP-08, results showed that the soils contain very high concentrations of transuranic elements, whereas the concentration levels were low for fission products (e.g. ^{137}Cs) and activation products such as ^{60}Co and europium isotopes. Thus, it is assumed that the contaminating source should refer to a test with a high neutron yield, with a relatively low fission power, leading to significant dispersion of nuclear material with only slight involvement of soils from the detonating area. This is also supported by the data on the plutonium level in individual particles and the number of identified radioactive particles. The contamination associated with the HP-10 site belongs, however, to another nuclear event/experiment, in which the yield of nuclear reaction was high, since the concentrations of fissile material and fission products are comparable.

The appearance of the extracted particles varied significantly (Fig. 8). The most typical particle appeared as a melted black, matte or shiny entity or as conglomerates with non – melted soil particles. Very often, the particle appearance indicated no influence of high temperatures, although the ^{239} ^{240}Pu activity concentration could reach 5000 Bq per particle, i.e. ~2 μg Pu/particle. In this case, it can be assumed that ^{240} ^{239}Pu is included in such particles as micrometer sized inclusions.

3.1.4. Characterisation of individual particles

Based on light and electron microscopy with microanalysis, low activity particles (n 10, <0.1–4.5 Bq ^{137}Cs, <0.1 Bq ^{241}Am) collected from the Experimental Field (HP-4) were large and showed an irregular molten glassy appearance with visible vesicles on the exterior (Fig. 9).

Particles from Ground Zero (HP-10) appeared also as glassy, with non-porous surface sand greyish-black color. With the specific aim of establishing (a) which (amorphous and crystalline) phases are present in particles from the Experimental field site, (b) in which of these phases the actinide elements are present and (c) the spatial distribution and chemical state of these elements, three particles were subjected to a combination of different synchrotron radiation based X-ray microscopic methods, namely submicron resolution absorption X-ray tomography, confocal XRF mapping and microbeam XRPD/XRF tomography.

The absorption tomograms of the particles from site P2 (HP-08, Figs. 10–12) reveal that below the smooth and regular exterior, several phases of strongly different densities are present as well as quasi-circular vesicles (Figs. 10 and 11), e.g., similar to what has been reported for Trinitite material from the World's first nuclear detonation (Fahey et al., 2010; Holliday et al., 2017), for fallout particles from tower shots at Nevada test site (Miller, 1963; Crocker et al., 1966), and for ellipsoidal and transparent glassy fallout particles from British nuclear tests (Breakaway, Round 4, Maralinga; Mosaic G2, Monte Bello Island) in Australia (Salbu et al., 2018; Geckeis et al., 2019). This may reflect that these particles are formed by condensation/solidification from liquid/-gaseous state at high temperature and pressure. The most abundant material appears to be an amorphous, glassy phase in which a variety of trace metals are present, such as Fe, Cu, Zn, Ga etc. (Fig. 10d). The distribution of these metals within the glassy phase appears to be heterogeneous, supporting assumptions of rapid condensation and solidification of previously liquid material. At the interface between the glassy material and the vesicles, inclusions are visible that appears to be enriched with respect to the actinides U and Pu (white inclusions in Fig. 10c indicate high density material). This is another feature in common with observations from fallout particles from Australian tests (Salbu et al., 2018). At some positions, locally enriched concentrations of U and Pu, and related elements such as Zr, are also observed. According to Holliday et al. (2017), silica and alkali glasses in glassy fallout particles from the Trinity test are melting products, whereas the CaMgFe (mafic) glass formed by condensation of evaporated ground, structure, and device materials. Furthermore, plutonium from the weapon was most strongly associated with the mafic glass and excluded from felsic glass (SiO2) and inclusionary phases (Fahey et al., 2010; Holliday et al., 2017). From our data, it appears actinides are not associated with quartz or amorphous phases and may be associated with mafic glass as suggested by Holliday et al. (2017). The outer surface of the sphere appears different from the inner parts of the particle in the following ways: (a) no vesicles are visible from the outside; (b) the formation of a crystalline phase, Fe_3O_4 (magnetite) can be observed as a thin spherical layer of variable thickness coating of the particle, (c) the outer shell is enriched in trace metals such as Ga, Zn, Pb, Fe and Cu as well as in U and Pu. In one particular particle (Fig. 12), the actinides appear to be coexisting within the magnetite phase. In the other droplet-like particle (Fig. 11), U and Pu also coexist. However, only a small fraction of these actinides is located in the magnetite phase and are also not correlated with the quartz or the amorphous material.

Based on the observations, it seems reasonable to suggest that the glassy, Fe-rich, amorphous phase that makes up the bulk of the particle is influenced by surrounding soils, and that the particle surfaces are gradually crystallizing, possibly due to interaction with environmental agents such as moisture and oxygen, resulting in the formation of crystalline magnetite.

A third particle from Experimental Field (HP-08, Fig. 12) showed an irregular shape, with non-glassy surface, i.e., a different appearance compared to what was observed for other particles from the Ground zero. As seen in Fig. 12e, the particle containing 60 Bq ^{241}Am exhibited a dual correlation between U and Pu, one group with a Pu L/U L ratio of ~0.9 and another with a ratio of ~1.8. As also seen in Figs. 10–12, it appears U and Pu co-exist in all particles. However, in two of the particles (Figs. 11 and 12) they are not associated with neither quartz, magnetite nor amorphous phases.

In the particles from epicentres within the Experimental field being subjected to spatially resolved SR based XRDP/XRF analysis, U and Pu are highly correlated (Fig. 12e), similar to that observed at other contaminated sites (e.g., Tel'kem I and II at STS, Palomares, Thule and McGuire Air Force Base), previously determined for actinide containing

Table 2
Activity concentration of radionuclides (Bq/kg std dev) in bulk soil samples.

Sample	^{239} ^{240}Pu Bq/g	^{241}Am Bq/kg	^{137}Cs Bq/kg	^{60}Co Bq/kg	^{152}Eu Bq/kg	^{154}Eu Bq/kg	^{155}Eu Bq/kg
HP-08	13100 750	1,750,000 100,000	2300 130	86 9	1510 70	<13	<9
HP-09	11,3 1,2	840 110	1130 90	195 15	4500 45	180 8	<10
HP-10	46,9 2,4	2400 160	21000 600	83 8	2500 80	92 5	46 9

Table 3
Average number of particles per gram of each fraction (N), and average activity concentration of ^{240} ^{239}Pu (Bq) per particle (A).

Sampling point	Fraction 1[a]		Fraction 2[b]		Fraction 3[c]		Fraction 4[d]	Fraction 5[e]
	N	A	N	A	N	A	N	N
HP-08	22	3600	60	1300	24	100	560	12,540
HP-09	1.2	4.9	6,2	1.5	29	<0.2	54	167
HP-10	12	2.2	30	0.77	66	0.23	10	10

[a] Fraction 1 (>1250 μm).
[b] Fraction 2 (1250-500 μm).
[c] Fraction 3 (500-280 μm).
[d] Fraction 4 (280–112 μm).
[e] Fraction 5 (112 - 40 μm).

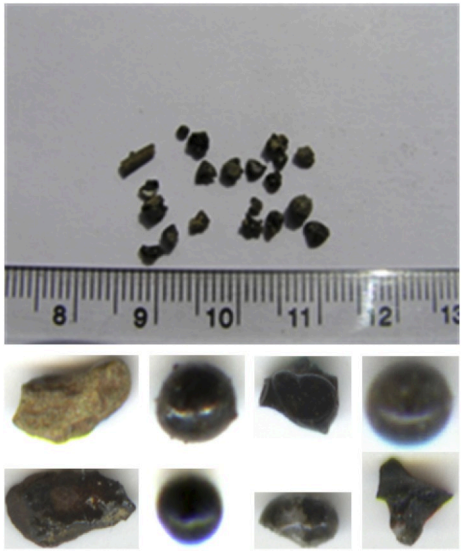

Fig. 8. Radioactive particles extracted from soils collected within Experimental Field (Lukashenko et al., 2017).

particles originating from nuclear weapon material (Geckeis et al., 2019; Lind, 2006; Lind et al., 2007).

Accelerator mass spectrometry (AMS) measurements of aqua regia leachates of the particle in Fig. 9b yielded a ^{240}Pu/^{239}Pu atom ratio of 0.040 0.009 (Lind, 2006), in agreement with the value of 0.0438 0.0001 reported by (Beasley et al., 1998) for a single surface soil sample collected at Ground Zero. AMS was also utilised to measure a ^{236}U/^{235}U atom ratio of 0.00036 0.00004 in this sample, which is significantly higher than those of natural U (Lind, 2006).

3.2. Peaceful nuclear explosion (PNE) - Atomic Lake

At present, the maximum soil activity concentrations of ^{241}Am, ^{239} ^{240}Pu, ^{238}Pu, ^{137}Cs, ^{90}Sr, ^{152}Eu, and ^{154}Eu in the vicinity of the Atomic Lake are 4000 Bq/kg, 17,000 Bq/kg, 7500 Bq/kg, 22,000 Bq/kg, 10,000 Bq/kg, 16000 Bq/kg, and 6000 Bq/kg, respectively. The main soil contamination was found close to the crater of the Atomic Lake, limited to 1–2 km downstream from the crater ridge. The level of contamination is significantly higher than global fallout levels (Lukashenko, 2017). Table 4 shows the activity concentration ranges of radionuclides in selected soil samples which were used to study the size distribution, mobility and potential bioavailability of radionuclides in the Atomic Lake area.

3.2.1. Size distribution of radionuclides

Enrichment factors describing the size distribution of radionuclides in different soil fractions are shown in Fig. 13. Results showed that the size distributions of radionuclides in soils, especially that of transuranics, varied with the composition of the fallout from nuclear tests. The results showed that there are two different size distribution patterns for the radionuclides observed in soil fractions at the Atomic Lake in that ^{137}Cs and to some extent ^{90}Sr are enriched in the fine soil fractions, while ^{241}Am and ^{239} ^{240}Pu are enriched in the coarse fractions.

3.2.2. Mobility and potential bioavailability of radionuclides

The fractions of ^{137}Cs, ^{239} ^{240}Pu and ^{241}Am in soils affected by the fallout plume were strongly associated with solids (^{137}Cs–98%, ^{239} ^{240}Pu – 97%, ^{241}Am–98%). The activity concentrations of ^{137}Cs present in water-soluble and organic forms was below the detection limits, the levels of ^{137}Cs in exchangeable form were insignificant and the fractions in mobile form (1.2–1.6%) were also low in soils affected by the fallout plumes. No change was observed with respect to the speciation of ^{137}Cs as a function of distance from the epicenter. The fractions of ^{239} ^{240}Pu present as organic (1.6%) and mobile (1.1%) forms were low as well. The concentration of ^{241}Am in mobile forms in

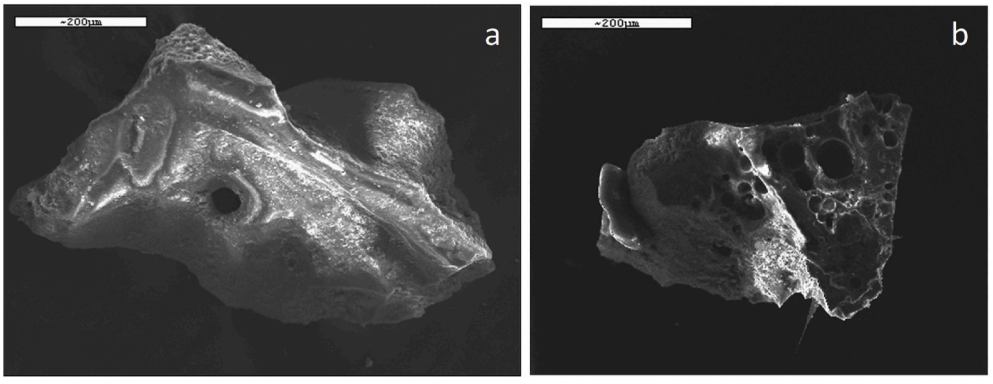

Fig. 9. Electron micrographs of vitrified radioactive particles isolated from the Experimental Field (HP-04). Scale bar 200 μm. The ^{236}U/^{235}U and ^{240}Pu/^{239}Pu atom ratios of the particle in (b) were determined by AMS (Lind, 2006). Fig. 9b is a reprint from the cited work (Lind, 2006).

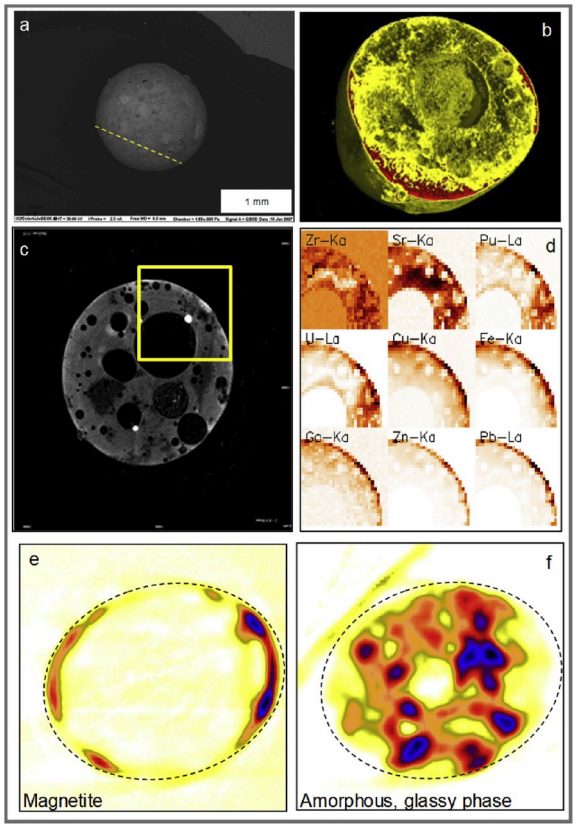

Fig. 10. Characterization of a 930 Bq ^{241}Am and 1200 μm diameter particle from the Experimental field HP-08, site P-2. (a) ESEM backscattered imaging micrograph, bar 1 mm, yellow dotted line marks the plane of the tomographic analysis in e) and f), (b) screen shot of 3D video rendering of nano-CT data, red and yellow indicate high and low density material, respectively, (c) nano-CT absorption tomogram based on density distribution, (d) element specific maps based on virtual slicing by means of confocal XRF planes through the approximate center-of-mass of the particle indicated by a yellow rectangle in c) (dimensions of map: 200 200 μm^2), (e–f) phase specific tomograms obtained by XRPD tomography (dimensions of map: 660 660 μm^2). (For interpretation of the references to color in this figure legend, the reader is referred to the Web version of this article.)

soils affected by the fallout plume was registered in only one sample (11%), while most of the ^{241}Am was strongly associated with solids. The lowest mobility of ^{90}Sr radionuclide was observed within the earth dump. A major fraction of ^{90}Sr was strongly associated with solids (53%), while the exchangeable fractions (26%) and the mobile fractions (19%) were significant. The water-soluble (1.9%) and organic (0.5%) fractions of ^{90}Sr were rather low. The mobility and potential bioavailability of ^{90}Sr was found to increase with distance from the epicenter along the plume axis. Fig. 14 demonstrates the increase in exchangeable and mobile forms, and the decrease in strongly associated ^{90}Sr in soils collected along the fallout plume, with increasing distance from the ridge of the Atomic Lake (Kunduzbayeva et al., 2017).

3.2.3. Presence of radioactive particles

Table 5 shows the activity concentration of radionuclides in soil samples, from which radioactive particles were isolated (Table 6). The particles collected at the Atomic Lake (Fig. S4), were isolated from sample HP-11, which was collected on the ridge (Table 5).

The molten form of the isolated particles was rather similar to particles isolated from soils collected at the Experimental Field, indicating particle formation at high temperatures and pressures. Almost all particles were droplet-shaped and spherical. However, it should be noted that the total number of detected "hot" particles is significantly less than in the Experimental field at a comparable concentration of transuranic elements. This is probably due to the temperature kinetics of the epicenter zones during excavation explosions, in which there is no long-duration relatively slow-cooling high-temperature zone.

3.3. Fallout from surface ground tests and global fallout (background) within STS

Table 7 shows the concentration ranges of radionuclides in the selected samples from the Southern plume believed to be contaminated by the fallout from the thermonuclear test in 1953, from the Southeast background sites which were probably affected both by the test and by global fallout, and from the Northern areas affected by global fallout only. These samples were used for studying the size distribution pattern, mobility and potential bioavailability of radionuclides.

The activity concentrations corresponding to the background level associated with global fallout in the STS territory are: ^{137}Cs–18, ^{90}Sr – 11, ^{241}Am - < 0.8, ^{239} ^{240}Pu – < 4 Bq/kg (Lukashenko, 2017), in accordance with data given for the Northern area.

3.3.1. Size distribution of radionuclides

The relative size distribution of radionuclides in soil fractions is given in Figs. 15 and 16. The size distribution of radionuclides of interest in soils affected by the plumes following aboveground tests was fundamentally similar to that observed in epicenter areas and plumes of low-yield nuclear tests (e.g., B-1) at the Experimental Field. Thus, in soils affected by the south-eastern plume enriched levels of radionuclides were observed in the 250–500 μm fractions, as seen for ^{137}Cs and ^{90}Sr, as well as in the fine soil fractions (Fig. 15). Enrichment of the fine fractions is expected to increase downstream for the epicenter. Enrichment of ^{241}Am and ^{239} ^{240}Pu in the 250–500 μm fraction showed also a rather clear distribution pattern, towards courser fractions. The enrichment observed for fractions 8–40 μm fraction reflected, however, that the soils were affected by overlapping fallout plumes from other tests contributing to contamination of the study area.

Enrichment of radionuclides in the fine soil fractions is characteristic of global fallout, as shown in Fig. 16. The distribution pattern in soils affected by global fallout is quite different from soils affected by nuclear tests, both close to the epicenters and far away within the plume. Deviations in the distribution pattern could be attributed to an influence from additional plumes from aboveground nuclear tests.

3.3.2. Mobility and potential bioavailability of radionuclides

The "south-eastern" area at STS has been impacted by both global fallout, similar to that of the "northern" STS territory, and fallout following the above ground thermonuclear test (400 kt yield) conducted 12.08.1953 at the Experimental Field (Lukashenko, 2010). Results show that the relative fraction of radionuclides in exchangeable and mobile forms of ^{137}Cs in soils is significantly lower in soils affected by nuclear fallout plumes compared to global fallout. The fraction of ^{137}Cs in exchangeable form in soils from the "south-eastern" area were a factor of 3 lower (from 2.4% to 0.74%), and the mobile form a factor of 3.5 lower (from 1.4% to 0.44%).The fractions of ^{239} ^{240}Pu assumed to be associated with organic compounds were, however, rather similar in the plume zone and in the territories. There is unfortunately no information on radionuclides associated with organics in the STS territory. In soils affected by the thermonuclear test plume, the fraction of ^{239} ^{240}Pu organically bound form, on average, was 0.75%. In the global fallout "background" area, the fraction was a factor of 2 higher (1.3%). This fact is consistent with data showing lower transfer of ^{239} ^{240}Pu to zonal plants growing in soils affected by the thermonuclear test fallout compared with soil affected by global fallout in the "south-eastern" STS area (Larionova et al., 2013). Although the uptake could possibly be attributed to the presence of organically bound form of ^{239} ^{240}Pu in soils, the radionuclides are predominantly strongly associated to the soil (>98%).

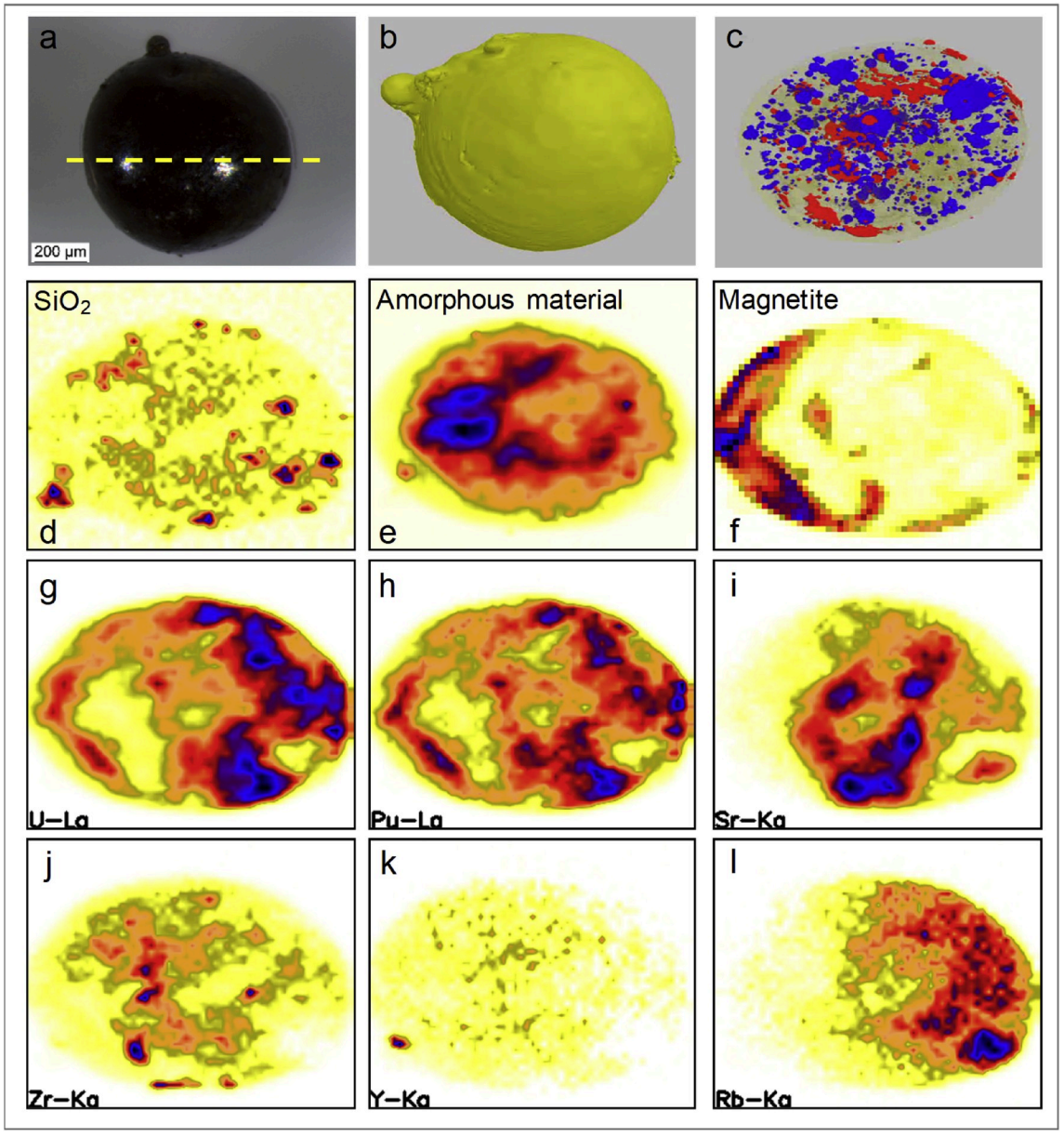

Fig. 11. Characterization of a 104 Bq ^{241}Am and 500 μm diameter particle from the Experimental field HP-08, site P-2. (a) Light microscopy, bar 200 μm, yellow dotted line marks the plane of the tomographic analysis, (b) video screen shot of 3D surface rendering of nano-CT data, (c) video screen shot of 3D transparent view rendering of nano-CT data showing the high (red) and intermediate (blue) density materials through the entire sample, (d–f) phase specific tomograms obtained by XRPD tomography, (g–l) element specific maps based on virtual slicing by means of XRF tomography through the approximate center-of-mass of the particle. (For interpretation of the references to color in this figure legend, the reader is referred to the Web version of this article.)

The fractions of exchangeable and mobile ^{90}Sr varied substantially with soils investigated. The fraction of the exchangeable form in the "northern" global fallout area is more than 60%, while the mobile fraction reached 17%, and the fraction strongly bound was less than 23%. The "south-eastern" STS area were also impacted by fallout from the above ground thermonuclear test, and the exchangeable fraction of ^{90}Sr decreased to 29%, with minimum level of the exchangeable form closest to the edge of the plume area. At these spots, data on radionuclide species vary significantly due to heterogeneity of the fallout from different sources. In soils significantly affected by the thermonuclear fallout, the fraction of ^{90}Sr strongly associated with solids was dominating, reaching 98%, close to what was observed at the Experimental Field. Thus, the ^{90}Sr exchangeable fraction in the "south-eastern" territory decreased by two orders of magnitude relative to background areas.

Detailed studies of the behavior of ^{90}Sr in soils affected by fallout from the thermonuclear test in the "south-eastern" territory has revealed that the fraction of exchangeable and mobile forms of ^{90}Sr increased with increasing distance from the explosion epicenter. Fig. 17 shows the variation of the exchangeable fraction of ^{90}Sr in soils affected by the 1953 thermonuclear test fallout as a function of the distance from the epicenter at P-1. The results are consistent with those obtained from uptake and accumulation of radionuclides by zonal plants in soils situated along the "plume" axis with increasing distance from the explosion epicenter (Larionova et al., 2013). Thus, information on ^{90}Sr species would reflect the contaminating sources; where the size distribution pattern and mobility and potential bioavailability would be very low in areas affected by nuclear test, while significantly higher if areas are affected by global fallout only (Lukashenko, 2010, 2012, 2015).

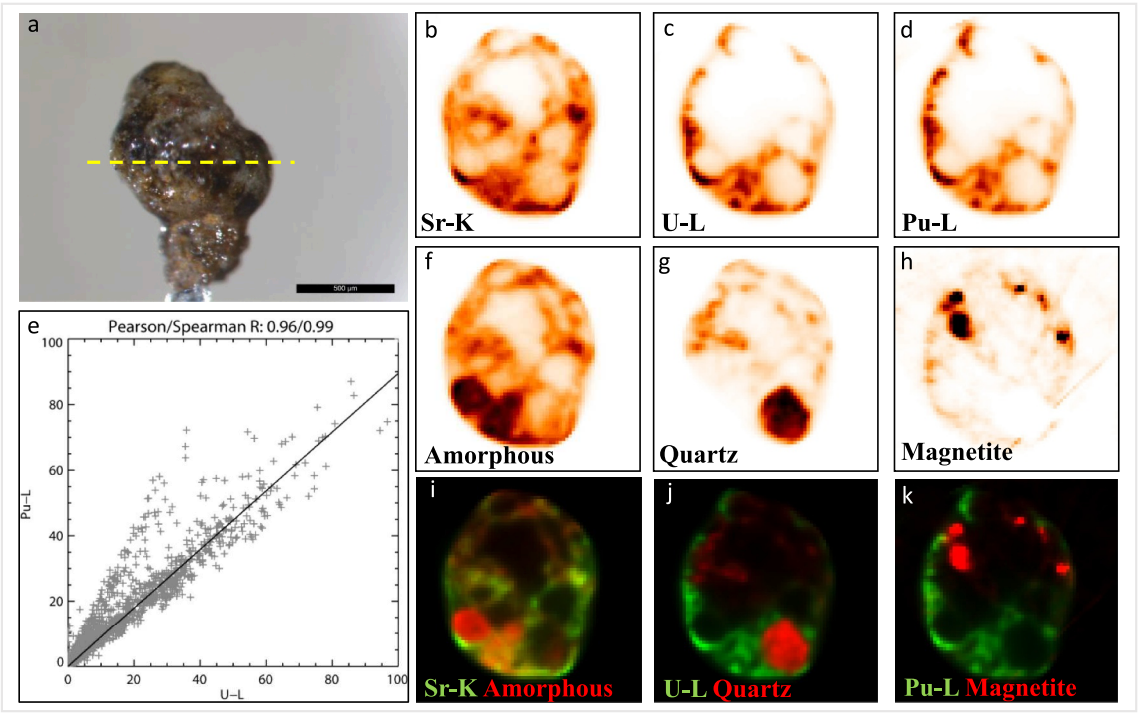

Fig. 12. Characterization of a 60 Bq ^{241}Am and 1.1 mm long particle from the Experimental field, site P-2 (HP-08). (a) Light microscopy of the particle mounted on a glass capillary with super glue, bar 500 μm, the yellow dotted line marks the plane of the tomographic analysis, (b–d) element specific maps based on virtual slicing by means of XRF tomography, (e) correlation plot of U La and Pu La based on the data in c) and d), (f–h) phase specific tomograms obtained by XRPD tomography at the same plane as in b-d, (g–i) element specific maps from (b–d) of Sr K, U La and Pu La superimposed on phase specific tomograms. (For interpretation of the references to color in this figure legend, the reader is referred to the Web version of this article.)

Table 4
Activity concentrations (Bq/kg) ranges of radionuclides in soil samples from the Atomic Lake.

Sample	Radionuclide			
	^{137}Cs	^{90}Sr	^{241}Am	^{239} ^{240}Pu
Atomic lake	30–13,800	10–11,000	10–670	220–5800

3.3.3. The presence of radioactive particles

Table 8 shows the activity concentration of radionuclides in soil samples, from which radioactive particles were isolated (Fig S5). The results reflect that all sampling points were influenced by radioactive fallout, as the activity concentrations of ^{137}Cs and transuranic elements exceeded the global fallout levels with a factor of more than 10 and 2 orders of magnitude, respectively. However, the levels are significantly lower than seen at epicenter zones.

As can be expected (Table 9), the number of large radioactive particles (size range 0.3–1 mm) in soils affected by fallout traces is approximately 2 orders of magnitude less than in soils from epicenter zones.

At the same time, the radioactive particles are associated with smaller fractions (0.04–0.3 mm), at some points the number of particles/sample is similar to that seen in soils from epicenter zones. The appearance of these radioactive particles seemed not to differ from particles observed at epicenter (e.g., conglomerates of molten and non-molten rock, or partially melted), although the frequency of finding particles is lower. Furthermore, the activity concentration of Pu/particle seemed also to be similar to those observed at epicenters.

3.4. Underground nuclear tests in tunnels at Degelen Mountain

Table 10 shows the activity concentration ranges of radionuclides in meadow soil samples from the tunnel entrance at the Degelen Mountain (Fig. 5), selected to study the size distribution, mobility and potential bioavailability of radionuclides.

3.4.1. Size distribution of radionuclides

The distribution of radionuclides in soil fractions is presented as enrichment factors (EF) in Fig. 18. The relative radionuclide distributions tended to increase in concentrations as the soil particle sizes decrease. This could imply that the radionuclide distribution could be attributed to sorption of radionuclides to soil particles, hence the radionuclide accumulation on particles should depend on the surface area of particles, their material composition and charge properties. Besides, the sorption rate is likely to depend on the properties of radionuclide species. For example, the enrichment factor for ^{239} ^{240}Pu in the <1 μm soil fraction is 2–3 times lower than for ^{137}Cs. The enrichment factor for ^{239} ^{240}Pu reached high values (EF 15) in the 63-40 μm fraction. This is most likely due not only to sorption processes, but also to co-precipitation with Fe or Mn, which can result in particles with properties completely different from particles produced by nuclear detonations.

3.4.2. Mobility and potential bioavailability of radionuclides

Unlike the size distribution of ^{137}Cs in soils from the Experimental Field, the distribution of ^{137}Cs in meadow soils at the Degelen Mountain site is characterized by higher fractions of exchangeable (1.8%) and mobile (1.9%) forms (Kabdyrakova et al., 2010). The ^{90}Sr in soils from the Degelen site is typically characterized by high mobility and potential bioavailability (exchangeable form 52%; mobile form 38%). The fraction of water-soluble form, found in virtually all samples, was 1.6%, while the fraction strongly associated to solid was 2.4%.

3.4.3. Presence of radioactive particle

Table 11 shows the activity concentrations of radionuclides in

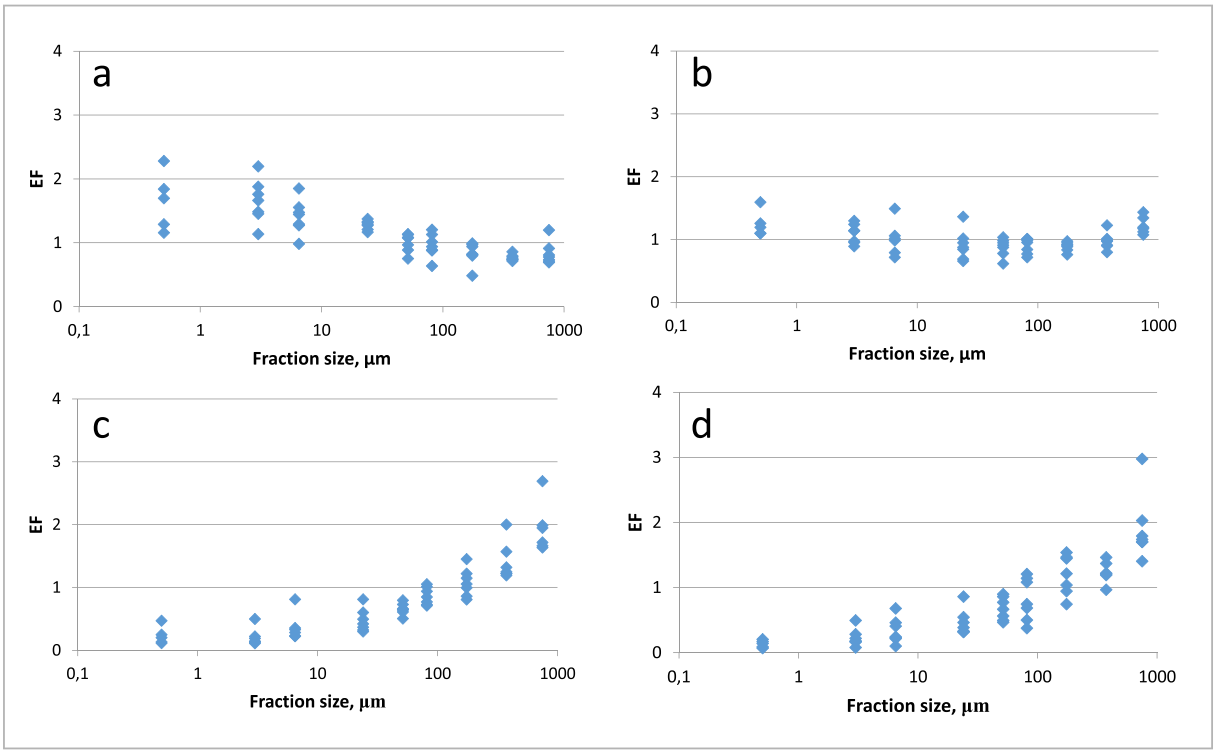

Fig. 13. Enrichment factor for ^{137}Cs (a), ^{90}Sr (b), ^{241}Am (c) and ^{239} ^{240}Pu (d) in soil fractions from the region of the Atomic Lake.

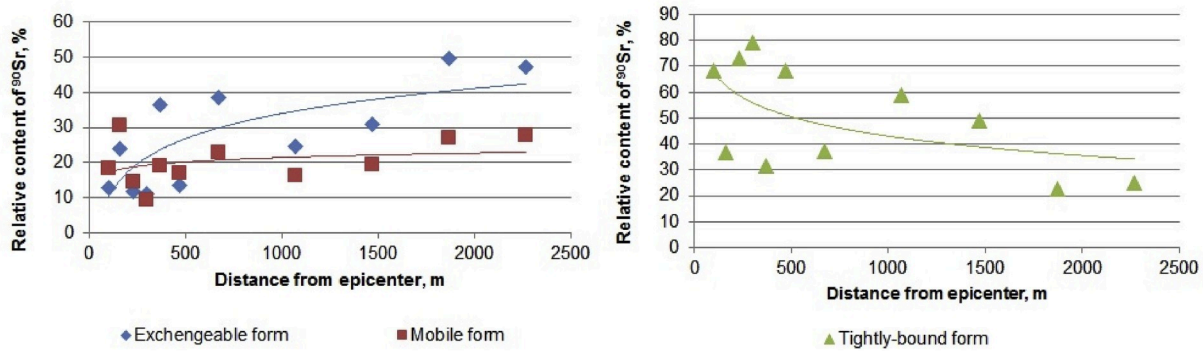

Fig. 14. Relative concentration of ^{90}Sr species in soils, as a function of distance from the Atomic Lake crater, along the axis of the fallout plume (Kunduzbayeva et al., 2017).

Table 5
Activity concentrations of radionuclides in bulk samples.

Sample	^{239} ^{240}Pu Bq/g	^{241}Am Bq/kg	^{137}Cs Bq/kg	^{60}Co Bq/kg	^{152}Eu Bq/kg	^{154}Eu Bq/kg	^{155}Eu Bq/kg
HP-11	11.2 1.4	1040 130	12,100 460	4000 400	7600 700	3600 360	67 9
HP-12	<0.39	21 2	540 20	91 10	198 15	83 5	

samples, from which radioactive particles were isolated (Table 12). As can be seen from the results (Tables 11, 12), soils from the different selected points differed significantly with respect to activity concentrations, number of particles in the soils and the Pu level in the particles, reflecting differences in the nuclear tests performed and processes taking place at present in these tunnels.

Point HP-16 refers to the tunnel N–139, a tunnel without penetrating water, and the contamination of the near-port site was associated with opening of the tunnel after the nuclear test to remove the radioactive residues. In appearance, non-melted particles with possible micrometer sized inclusions of nuclear substance (Fig. S6), the particles from tunnel 139 seemed similar to some particles found in soils from the epicenter zone (point HP-08).

The tunnels N– 177, 503 and 609 (points HP-19, HP-20 and HP-17, HP-18) are tunnels with water flowing from the tunnels into the surrounding surface environment. The activity concentrations of ^{137}Cs were high, in the range of n 10^2 - n 10^3 Bq/L, while the activity concentrations of transuranic elements were low (n 10^0 Bq/L). Since this process has lasted for many years, high concentrations of radionuclides have accumulated in the bottom sediments. The active particle fractions in samples from HP-17, HP-18 (tunnel 609) and HP-19 (tunnel 177) seemed to have an organic-mineral origin (Fig. S6). In the first case,

Table 6
Average number of particles per gram of each fraction (N), and average activity concentration of ^{240} ^{239}Pu (Bq) per particle (A).

Sample	Fraction 1[a]		Fraction 2[b]		Fraction 3[c]		Fraction 4[d]	Fraction 5[e]
	N	A	N	A	N	A	N	N
HP11	0.14	0.58	0.26	0.11			<1	<1
HP12	<0.01		<0.01		0.1	<0.01	<1	<1

[a] Fraction 1 (>1250 μm).
[b] Fraction 2 (1250-500 μm).
[c] Fraction 3 (500-280 μm).
[d] Fraction 4 (280–112 μm).
[e] Fraction 5 (112 - 40 μm).

Table 7
Activity concentrations ranges of radionuclides in soil samples from areas affected by plume fallout and by global fallout.

Venue	Radionuclides, Bq/kg			
	^{137}Cs	^{90}Sr	^{241}Am	^{239} ^{240}Pu
Southeastern plume, 12.08.1953	40–540	120–2400	0,6–6,0	10–120
Southeastern area, mixed sources zone	24–90	24–100	1,0–3,5	2,2 - 21
«Northern » area Global fallout	17–56	12–61	0,9–7,1	1,9 - 20

remains of wood material, grass and leaves were present, in the second case the particles were observed as fragile amorphous organo-mineral conglomerates. The presence of such particles confirms the assumption of sorption, co-precipitation and possibly the formation of secondary minerals enriched in radionuclides.

3.5. Linking particle characteristics to specific sources

The first test at STS was performed in 1948, initiating the weapon program of the Soviet Union. A total of 456 nuclear tests have been conducted, in the atmosphere, on surface ground and underground. In addition to the testing of weapons purposes, peaceful nuclear explosions were performed for civil purposes such as excavation of the Atomic Lake. Within the Experimental field, a series of sources have been detonated, and a series of plumes are still affecting the territory. It is, however, believed that the physico-chemical forms of radionuclides, in particular the presence of radioactive particles, in soils from STS will depend on the source (i.e., specific tests), on the conditions under which they were formed (surface or ground tests), and on transformation processes taking place in the environment during the time that has passed since the tests were conducted (aging). It is believed that radionuclides released from different tests have different properties and will behave differently in the ecosystem. Thus, a key issue is to link specific sources to particle characteristics such as particle size distribution, and mobility, as well as 2- and 3- dimensional information on structures and compositions.

In the present work, collected soils samples have been targeted to specific sources, and efficient particle size screening using enrichment factors was used to localize particles. Furthermore, sequential extractions were applied to estimate the mobility potential and potential bioavailability of relevance for ecosystem transfer of particle associated radionuclides. Based on available samples, the particle size distributions of radionuclides (^{137}Cs, ^{90}Sr, Pu-isotopes, ^{241}Am) in soils from STS were determined based on wet sieving followed by calculation of the relative soil fractions being enriched. Results show that the relative radionuclide size distribution depended on the source and released scenarios. In soils

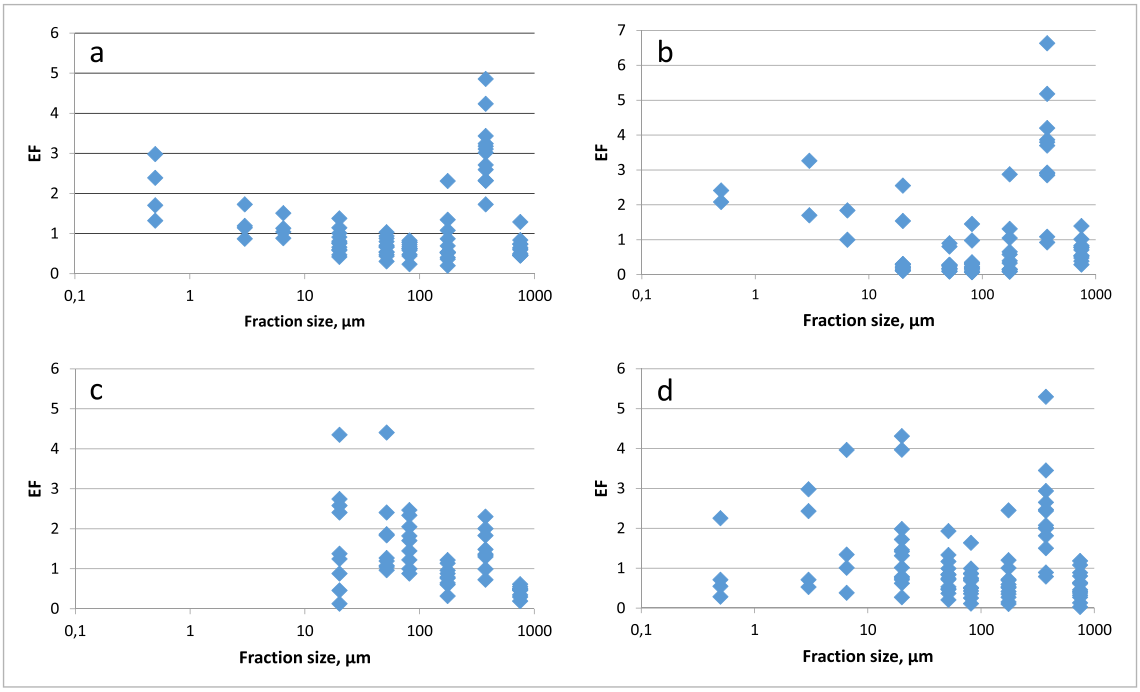

Fig. 15. Enrichment factors for ^{137}Cs (a), ^{90}Sr (b), ^{241}Am (c) and ^{239} ^{240}Pu (d) in soil fractions affected by the plume from the above ground thermonuclear test at 12.08.1953.

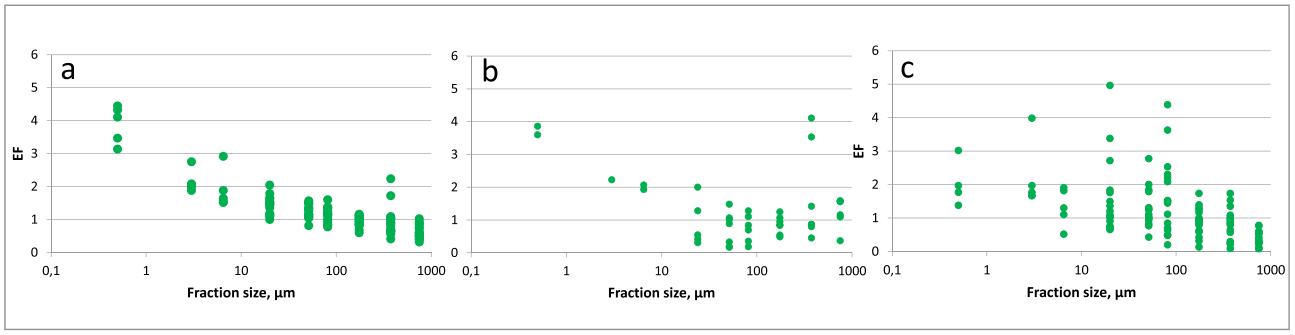

Fig. 16. Enrichment factor for a) ^{137}Cs, b) ^{90}Sr and c) ^{239} ^{240}Pu in soil fractions from areas affected by global fallout (background, south-eastern area) within the STS territory.

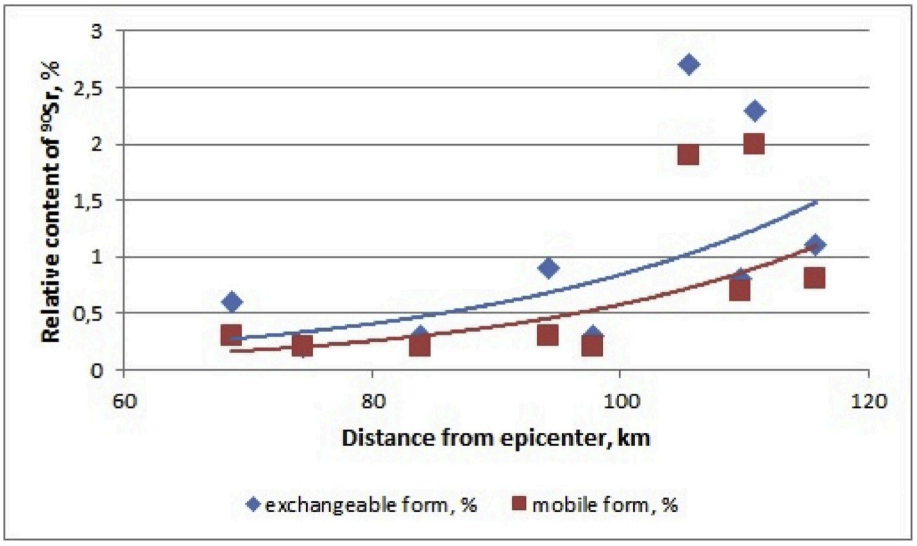

Fig. 17. Variation in the relative fraction (%) of exchangeable and mobile forms of ^{90}Sr in soils as a function of distance from the explosion epicenter (Lukashenko et al., 2017).

Table 8
Activity concentrations of radionuclides in bulk samples areas of surface ground tests and global fallout (background).

Sample	^{239} ^{240}Pu mBq/kg	^{241}Am Bq/kg	^{137}Cs Bq/kg	^{60}Co Bq/kg	^{152}Eu Bq/kg	^{154}Eu Bq/kg	^{155}Eu Bq/kg
HP-01	3.7 1.1	450 140	79.6 8,0	<3	<2	<1.8	<2
HP-02	1.6 0.3	97 17	710 130	<1,1	6.4 1.2	<1.2	3.7 0.5
HP-03	2.9 1.8	122 38	260 174	<5	13 3	<3	8 2
HP-04	11 2	1190 210	962 60	<5	158 13	7 3	10 2
HP-05	3.2 1.4	136 27	172 42	<2	14 3	<2	<2
HP-06	1.3 0.2	105 12	440 60	<3	4 2	<2	2.6 0.4

affected by radioactive particles, results showed also that the major part of radionuclides was enriched in defined particle-size fractions of soils. Then, advanced SEM, XRF and synchrotron radiation x-ray based micro-techniques could be utilised for detailed 2D and 3D particle characterization issues, also reflecting formation mechanisms.

At the Experimental Field, radionuclides in soils from epicenters affected by fallout from surface nuclear tests were mainly enriched in the coarse soil fractions with diameter larger than 250–500 μm and larger size fractions for transuranics than for ^{137}Cs and ^{90}Sr. Following nuclear detonation, refractory elements are believed to be retained in the course matrix particle, while such particles would be depleted with respect to more volatile elements having gaseous precursors such as Cs and Sr. In remote areas of plumes from aboveground nuclear tests, however, the enriched fractions decreased in size with distance from the epicenters. In areas believed to represent global fallout only, the major fraction enriched in radionuclides occurred in the fine-dispersed soil fractions with diameter less than 1 μm. In addition, transformation processes may occur in the environment as observed in sediments from the outlet creek from the Degelen mountain. Here, particle formation is attributed to sorption, co-precipitation with Fe-elements as well as the formation of secondary minerals.

Based on sequential extraction, the radionuclide species in soils contaminated by fallout from aboveground nuclear explosions from the Experimental Field (Fig. 2) are characterized by low mobility and low potential bioavailability. The predominant fraction of radionuclides was shown to be strongly associated to solid phases and would most probably be quite inaccessible to plants (i.e., ^{137}Cs – more than 99% associated with solid, ^{239} ^{240}Pu – 99% ^{241}Am – more than 90%, ^{90}Sr – 91%). In soils

Table 9
Average number of particles per gram of each fraction (N), and average activity concentration of ^{240} ^{239}Pu (Bq) per particle (A).

Sampling point	Fraction 1[a]		Fraction 2[b]		Fraction 3[c]		Fraction 4[d]	Fraction 5[e]
	N	A	N	A	N	A	N	N
HP1	0.01	0.45	<0.01		<0.01		–	–
HP2	0.03	13	0.65	1.6	2.4	0.35	<1	<1
HP3	0.02	53	<0.1		14	0.1	2	23
HP4	0.26	2	2.4	3.2	6.7	1.9	2	20
HP5	0.05	1.9	0.05	0.2	2.7	0.6	2.6	2.9
HP6	<0.01		0.9	1.2	4.5	0.4	<1	46

[a] Fraction 1 (>1250 μm).
[b] Fraction 2 (1250-500 μm).
[c] Fraction 3 (500-280 μm).
[d] Fraction 4 (280–112 μm).
[e] Fraction 5 (112 - 40 μm).

Table 10
Activity concentrations of radionuclides in meadow soils at Degelen Mountain (tunnel 176).

Venue	Radionuclide, Bq/kg			
	^{137}Cs	^{90}Sr	^{241}Am	^{239} ^{240}Pu
Tunnel 176	9500–87,000	22,000–48,000	<10	30–70

from the epicenter of the Experimental Field, the mobile fraction and the potential bioavailability of Cs-species were rather insignificant (^{137}Cs 0.6% and 0.3%). The assumed fractions of ^{239} ^{240}Pu in organic and mobile forms were up to 0.1% and 0.4%, respectively, while the fraction of ^{241}Am present in mobile forms reached 8.0%. Among the studied radionuclides in soils from the Experimental field, ^{90}Sr had the greatest migration capacity in soils at a given site, as the extracted fractions of ^{90}Sr reached 6.0% and mobile fractions reached 2.8%. Following the plume from the most powerful thermonuclear test (400 kt, 1953)

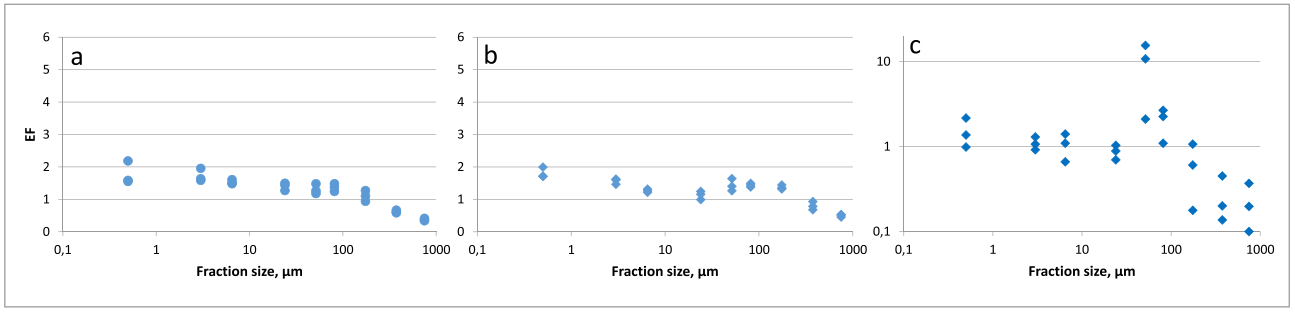

Fig. 18. Enrichment factor for ^{137}Cs (a), ^{90}Sr (b) and ^{239} ^{240}Pu (c) distribution in soil fractions at the tunnel 176 stream flow.

Table 11
Activity concentration of radionuclides in bulk sample.

Sample	^{239} ^{240}Pu mBq/kg	^{241}Am Bq/kg	^{137}Cs Bq/kg	^{60}Co Bq/kg	^{152}Eu Bq/kg	^{154}Eu Bq/kg	^{155}Eu Bq/kg
HP-16	515 100	42,300 8400	135 5	<3	4 2	<1.4	<3
HP-17	<3.6	128 14	302,000 16300	<16	<44	<32	<42
HP-18	<12	<87	4,490,000 67000	<48	<164	<136	<155
HP-19	16.0 1.2	583 53	4790 90	<21	<16	<13	<16
HP-20	<0,20	<1,2	49 5	<3	<3	<2	1,8 1,0

Table 12
Average number of particles per gram of each fraction (N), and average activity concentration of ^{240} ^{239}Pu (Bq) per particle (A).

Sample	Fraction 1[a]		Fraction 2[b]		Fraction 3[c]		Fraction 4[d]	Fraction 5[e]
	N	A	N	A	N	A	N	N
HP-16	2,2	0,085	1,2	0,46	4	0,052	29	125
HP-17	6,4	<0,01	<0.01		<0.02		320	41
HP-18	33	<0,025	<0.01		<0.02		4500	420
HP-19	9,7	0,05	<0.01		<0.02		125	<1
HP-20	1	<0,015	1,1	0,11	15	0,06	50	165

[a] Fraction 1 (>1250 μm).
[b] Fraction 2 (1250-500 μm).
[c] Fraction 3 (500-280 μm).
[d] Fraction 4 (280–112 μm).
[e] Fraction 5 (112 - 40 μm).

conducted STS, the fraction of exchangeable and mobile forms of ^{90}Sr observed along the fallout trails increased with distance from the epicenter of the conducted test. In contrast, the fractions of ^{90}Sr in mobile forms were significantly higher in the plume far from the epicenter.

The distribution of radionuclide species in soils at the Atomic Lake resembled that of the Experimental Field, as the formation of radioactive particles seems similar to processes following aboveground tests as well as underground explosions with soil ejection. The fractions of ^{137}Cs in extractable and mobile forms (1.4% and 1.2%) and the fractions of $^{239\ 240}$Pu in assumed organic (1.6%) and mobile (1.1%) forms were low. The distribution of ^{90}Sr was non-uniform, and the fraction of exchangeable and mobile forms in soils increased with distance from the epicenter of the explosion, similarly to fallouts trail which spans through the territory of the southeastern part of the assumed background territories of the STS.

Despite the higher levels of radionuclides in soil, the distribution of radionuclide species in soils at the Degelen Mountain was similar to the assumed background territories of the STS (global fallouts). The main fraction of ^{137}Cs was strongly associated to solid, while the exchangeable (52%) and the mobile (38%) fraction of ^{90}Sr in soils from Degelen was higher that at the Experimental Field, and close to what is obtained at the background territories affected by global fallout. Thus, independent of the particle formation processes and the particle properties, sequential extraction results showed that the mobility of ^{137}Cs and $^{239\ 240}$Pu were very low in the STS soils, especially at the epicenters. In contrast to the other radionuclides, ^{90}Sr showed the highest mobility in the STS soils, increasing with distance from the epicenter along the plume. Thus, changes radionuclide speciation, especially the ^{90}Sr species, from the retention in particle to particle weathering and remobilization, could be applied as a source indicator, differentiating between fallout plumes from different above-ground explosions.

In the present work, radioactive particles were found in almost all investigated STS samples. During high yield ground nuclear tests and excavation explosions (e.g., Atomic lake), the majority of radioactive particles are teardrop-shaped with melted surface. However, different kinds of particles were also detected at the epicenters, such as non-melted soil mineral particles containing significant amounts of plutonium, assumed being present as micrometer sized inclusions. The number of large radioactive particles with sizes 0.3 - > 1 mm was most frequently seen at epicenter zones, and the frequency decreased sharply with the distance from the epicenter. The number of smaller particles (0.04–0.3 mm) remained significant at a distance from the epicenters up to 5 km. Apparently, the presence of such particles explains the significant enrichment of radionuclides in the 0.2–0.5 mm fractions from contaminated soils collected even at tens of kilometers away from the epicenter of the nuclear explosion. At the Degelen site, no “typical” radioactive particles were identified in the bottom sediments of the flow-through water at the entrances of tunnels. However, plutonium was highly enriched (more than 10 times) in specific soil fractions in the bottom sediments, which is attributed to sorption, co-precipitation and possibly the formation of a secondary mineral.

4. Conclusions

In the present work, it seems that a significant part of the artificial radioactivity observed within the STS, especially at the epicenters of nuclear explosions, is contained in radioactive particles. The results suggest that four fundamentally different types of “hot particles are present:

Spherical particles with a generally shiny glazed, melted surface. A detailed study showed an internal porous structure, and surface layers enriched in transuranics. Such particles are frequently observed at epicenters of the explosions. The particles are probably formed by melting of rocks with subsequent crystallization and simultaneous sorption of radionuclides, in some cases condensation and crystallization from the gas phase;

Vitrified irregular particles observed at Ground Zero (HP-04), i.e., epicenter of several detonations. Such particles seem part of debris from the nuclear device as well as with interactions from soil components;

Soil particles with visually unchanged structure, with micrometer sized inclusions of actinides, which was confirmed by the study of the microstructure of such particles. Most often such particles are also found at epicenters;

Particles with amorphous structure found in bottom sediments of streams flowing from the tunnels at the Degelen Mountain. The activity of these particles can exceed the radioactivity of the surrounding soils by orders of magnitude. The appearance of such particles and the isotopic ratios lead to the conclusion that these particles could be formed as secondary minerals. Most likely, sorption and co-precipitation of transuranic elements with oxides and hydroxides of iron and manganese are involved, and such formation processes would be extremely interesting for future research.

Most particles identified at epicenters are relatively large, containing substantial radioactivity. The size and activity of the particles decreased along the plume with distance from the epicenters. In almost all cases ^{137}Cs, ^{241}Am, $^{239\ 240}$Pu in soils were strongly associated with solid phases (90–99%), while ^{90}Sr exhibited much greater variability as the mobility of ^{90}Sr varied with tests conducted and increased by distance from the epicenters.

Declaration of competing interests

The authors declare that they have no known competing financial interests or personal relationships that could have appeared to influence the work reported in this paper.

Acknowledgments

This work was supported by the Research Council of Norway through its Centres of Excellence funding scheme, project number 223268/F50, the RFBR, research project N_19-016-00146\19 as well as the International Atomic Energy Agency’s Coordinated Research Project K41013 “Environmental Behavior and Potential Biological Impact of Radioactive Particles”.

Appendix A. Supplementary data

Supplementary data to this article can be found online at https://doi.org/10.1016/j.jenvrad.2020.106160.

References

Beasley, T.M., Kelley, J.M., Orlandini, K.A., Bond, L.A., Aarkrog, A., Trapeznikov, A.P., Pozolotina, V.N., 1998. Isotopic Pu, U, and Np signatures in soils from semipalatinsk-21, Kazakh republic and the southern urals, Russia. J. Environ. Radioact. 39, 215–230.

Bunzl, K., 1997. Probability for detecting hot particles in environmental samples by sample splitting. Analyst 122, 653–656.

Crocker, G.R., O’Connor, J.D., Freiling, E.C., 1966. Physical and radiochemical properties of fallout particles. Health Phys. 12, 1099–1104.

De Nolf, W., Janssens, K., 2010. Micro X-ray diffraction and fluorescence tomography for the study of multilayered automotive paints. Surf. Interface Anal. 42, 411–418.

Fahey, A.J., Zeissler, C.J., Newbury, D.E., Davis, J., Lindstrom, R.M., 2010. Postdetonation nuclear debris for attribution. Proc. Natl. Acad. Sci. U. S. A. 107, 20207–20212.

Falkenberg, G., Rickers, K., Bilderback, D.H., Huang, R., 2004. A Single-bounce Capillary for Focusing of Hard X-rays, HASYLAB annual report 2003. HASYLAB, Hamburg.

Geckeis, H., Zavarin, M., Salbu, B., Lind, O.C., Skipperud, L., 2019. Environmental chemistry of plutonium. In: Clark, D.L., Geeson, D.A., Hanrahan, R.J. (Eds.), Plutonium Handbook, 2 ed. American Nuclear Society, pp. 1979–2118.

Gorlachev, I.D., Kvochkina, T.N., Knyazev, B.B., Lukashenko, S.N., 2011. Studies and systematization of hot particles in soils of Semipalatinsk Test Site. Issue 3. In: Topical Issues in Radioecology of Kazakhstan, vol. 2. Pavlodar.

GOST 12536-14 Soils. Methods of Laboratory Granulometric (Grain-size) and Microaggregate Distribution, 2015. Standartinform, Moscow (in Russian).
Holliday, K.S., Dierken, J.M., Monroe, M.L., Fitzgerald, M.A., Marks, N.E., Gostic, R.C., Knight, K.B., Czerwinski, K.R., Hutcheon, I.D., McClory, J.W., 2017. Plutonium segregation in glassy aerodynamic fallout from a nuclear weapon test. Dalton Trans. 46, 1770–1778.
IAEA, 2011. Radioactive Particles in the Environment: Sources, Particle Characteristics and Analytical Techniques. IAEA-TECDOC 1663. IAEA, Vienna, p. 90.
Janssens, K., Proost, K., Falkenberg, G., 2004. Confocal microscopic X-ray fluorescence at the HASYLAB microfocus beamline: characteristics and possibilities. Spectrochim. Acta B At. Spectrosc. 59, 1637–1645.
Kabdyrakova, A.M., Kunduzbayeva, A.Ye, Lukashenko, S.N., 2010. Species of radionuclide in soils of watercourse ecosystems at Degelen massif. In: Lukashenko, S. N. (Ed.), Proceedings of the Institute of Radiation Safety and Ecology over 2007-2009, vol. 2. Printing House, Pavlodar, pp. 273–286.
Kunduzbayeva, A.Ye, Lukashenko, S.N., Magasheva, R.Yu, 2013. Speciation of artificial radionuclides in soils of the testing ground “Experimental Field”. In: Lukashenko, S. N. (Ed.), Proceedings of the National Nuclear Center of the Republic of Kazakhstan over 2011-2012, vol. 2. Printing House, Pavlodar, pp. 173–198. Iss. 4.
Kunduzbayeva, A.Ye, Kabdyrakova, A.M., Larionova, N.V., Lukashenko, S.N., 2017. Speciation of artificial radionuclides in soils of the "Atomic lake" site at the Semipalatinsk test site. Radiation biology. Radioecology 4, 399–413 (in Russian).
Larionova, N.V., Lukashenko, S.N., Yankauskas, A.B., Ivanova, A.R., 2013. Radionuclides transfer from soil to plants in the area of radioactive fallout during the passage of the radioactive cloud (“plume” of the 1953 explosion). In: Lukashenko, S.N. (Ed.), Proceedings of the National Nuclear Center of the Republic of Kazakhstan over 2011-2012, vol. 2. Printing House, Pavlodar, pp. 153–159. Iss. 4.
Lind, O.C., 2006. Characterisation of Radioactive Particles in the Environment Using Advanced Techniques, PhD Thesis. Norwegian University of Life Sciences, Ås, pp. 1–191.
Lind, O.C., Salbu, B., Janssens, K., Proost, K., Garcia-Leon, M., Garcia-Tenorio, R., 2007. Characterization of U/Pu particles originating from the nuclear weapon accidents at Palomares, Spain, 1966 and Thule, Greenland, 1968. Sci. Total Environ. 376, 294–305.
Lind, O.C., De Nolf, W., Janssens, K., Salbu, B., 2013. Micro-analytical characterisation of radioactive heterogeneities in samples from Central Asian TENORM sites. J. Environ. Radioact. 123, 63–70.
Lukashenko, S.N., 2010. Topical issues in radioecology of Kazakhstan. In: Radioecological State of the “Northern” Part of Semipalatinsk Test Site Territory. Printing House, Pavlodar. Iss. 1.
Lukashenko, S.N., 2012. Radiation Safety Assurance in the Territory of the Republic of Kazakhstan, Annual (Informational) Report on Republican Budget Program 005 under the Contract No. 2/3 20.02.2012. IRSE NNC RK, Kurchatov (in Russian).
Lukashenko, S.N., 2017. Topical Issues in Radioecology of Kazakhstan. Optimization of Study of the Semipalatinsk Test Site Lands for the Purpose of Their Transfer into Economic Turnover, Dom Pechati, Issue 5. Kurchatov.
Lukashenko, S.N., Batyrbekov, E.G., Strilchuk, YuG., Umarov, M.A., Krivitskiy, P.E., Aidarkhanov, A.O., Panitskiy, A.V., Aktaev, M.R., Aidarkhanova, A.K., Larionova, N. V., YakovenkoYu, Yu, Subbotin, S.B., Turchenko, D.V., Lyakhova, O.N., Romanenko, V.V., Koigeldinova, M.T., BaigazinovZh, A., 2017, third ed.. Semipalatinsk Test Site. Present State. Press House, Pavlodar.
Miller, C., 1963. Fallout and Radiological Countermeasures, vol. 1, p. 402.
Nazarbayev, N.A., Shkolnik, V.S., Batyrbekov, E.G., Berezin, S.A., Lukashenko, S.N., Skakov, M.K., 2016. Performing Scientific and Technical, Engineering Works to Secure the Former Semipalatinsk Test Site, V. 2. Dom Pechati, Kurchatov (in Russian).
Pavlotskaya, F.I., 1974. Migration of Radioactive Products of Global Fallout in Soils. Atomizdat, Moscow, p. 215 (in Russian).
Ponomaryova, V.V., Plotnikova, T.A., 1980. Humus and Soil Formation (Methods and Study Results). Nauka, Leningrad (in Russian).
Salbu, B., Kashparov, V., Lind, O.C., Garcia-Tenorio, R., Johansen, M.P., Child, D.P., Roos, P., Sancho, C., 2018. Challenges associated with the behaviour of radioactive particles in the environment. J. Environ. Radioact. 186, 101–115.
Salbu, B., Lind, O.C., 2020. Analytical techniques for characterizing radioactive particles deposited in the environment. J. Environ. Radioact. 211, 106078.